

## Supporting Information

# **Direct Endgroup Modification of Poly(Aib)-polymers: Heterogeneous Peptide Coupling and Chiral Folding**

Sandipan Roy,<sup>a</sup> Christian Hildebrand,<sup>a</sup> Matthias Rohmer,<sup>a</sup> Yishen Xie,<sup>b</sup> Jitul Deka,<sup>b</sup> Justus F. Thümmel<sup>a</sup> and Wolfgang H. Binder<sup>\*a</sup>

Martin-Luther University Halle-Wittenberg, Chair of Macromolecular Chemistry, D-06120 Halle, Germany

## Contents

Synthesis Procedures.....	3
Synthesis of Aib-NCA .....	3
ROP of Aib-NCA using chiral initiators (A*, B*, C*) to prepare parent polymers.....	4
General Procedure for End-Group modifications of Poly(Aib) .....	4
Synthesis and Chiral Resolution of Feringa Photoswitches: (2R, 2'R, Z)-2,2',4,4',7,7'-hexamethyl-2,2',3,3'-tetrahydro-[1,1'-biindenylidene]-6,6'-diol (C <sup>R</sup> ) and (2S, 2'S, Z)-2,2',4,4',7,7'-hexamethyl-2,2',3,3'-tetrahydro-[1,1'-biindenylidene]-6,6'-diol (C <sup>S</sup> ): .....	5
Step 1: Synthesis of 6-methoxy-2,4,7-trimethyl-2,3-dihydro-1H-inden-1-one .....	5
Step 2: Synthesis of 6,6'-dimethoxy-2,2',4,4',7,7'-hexamethyl-2,2',3,3'-tetrahydro-1,1'-biindenylidene .....	6
Step 3: Synthesis of 2,2',4,4',7,7'-hexamethyl-2,2',3,3'-tetrahydro-[1,1'-biindenylidene]-6,6'-diol.....	7
Optical Resolution.....	7
NMR Analysis.....	9
NMR Analysis of Aib-NCA monomer .....	9
NMR Analysis of End-Group Modified Polymers.....	15
GPC Analysis .....	19
MALDI-TOF Analysis.....	20
Sensitivity Analysis.....	20
End-group Conversion Calculation .....	22
MALDI-TOF MS Spectra and Simulations of Parent Polymers .....	23
MALDI-TOF MS Spectra and Simulations of Modified Polymers .....	28
CD Data.....	46
AFM Data.....	48
XPS Data .....	48
Workflow for Gold Substrate Coating .....	50
CD Multivariate SSE Analysis.....	50
References .....	52

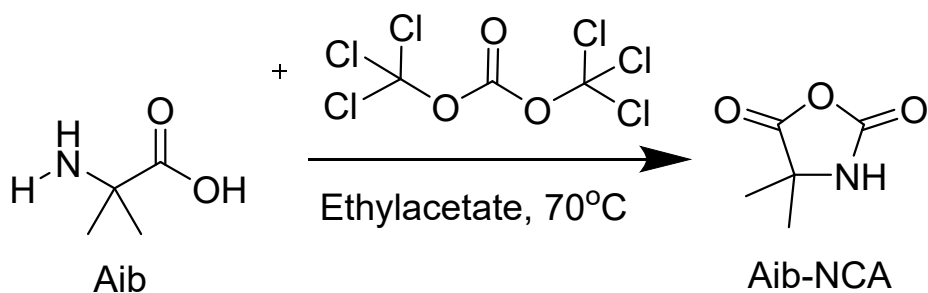
## Synthesis Procedures

### Synthesis of Aib-NCA

Aib-NCA was synthesized using a previously published procedure<sup>1</sup>. Aib (15.4 g, 0.175 mol, 1.0 eq) and  $\alpha$ -pinene (48.16 g, 0.353 mol, 2.37 eq) were suspended in dry ethyl acetate (170 mL). Triphosgene (35.5 g, 0.119 mol, 0.80 eq) was then added, and the suspension was heated to 70 °C until the mixture turned clear (approximately 24 h). The reaction was maintained for an additional 5 h to ensure complete consumption of residual triphosgene. After cooling to room temperature, excess HCl and phosgene were removed by purging with nitrogen and trapping in an aqueous NaOH solution. The solvent was evaporated under reduced pressure, and the crude product was recrystallized three times from an ethyl acetate/n-hexane mixture (1:10). The solid was collected by filtration and dried under vacuum to afford Aib-NCA as a white crystalline powder (12.8 g, 66%).

<sup>1</sup>H NMR (402 MHz, dmsO)  $\delta$  9.12 (s, 1H), 3.34 (s, 2H), 1.42 (s, 6H).

<sup>13</sup>C-APT NMR (101 MHz, dmsO)  $\delta$  174.63, 150.38, 59.27, 40.14, 39.94, 39.73, 39.52, 39.31, 39.10, 38.90, 24.66.



*SI 1: Synthesis of Aib-NCA using triphosgene and Aib at 70 °C for 3 days*

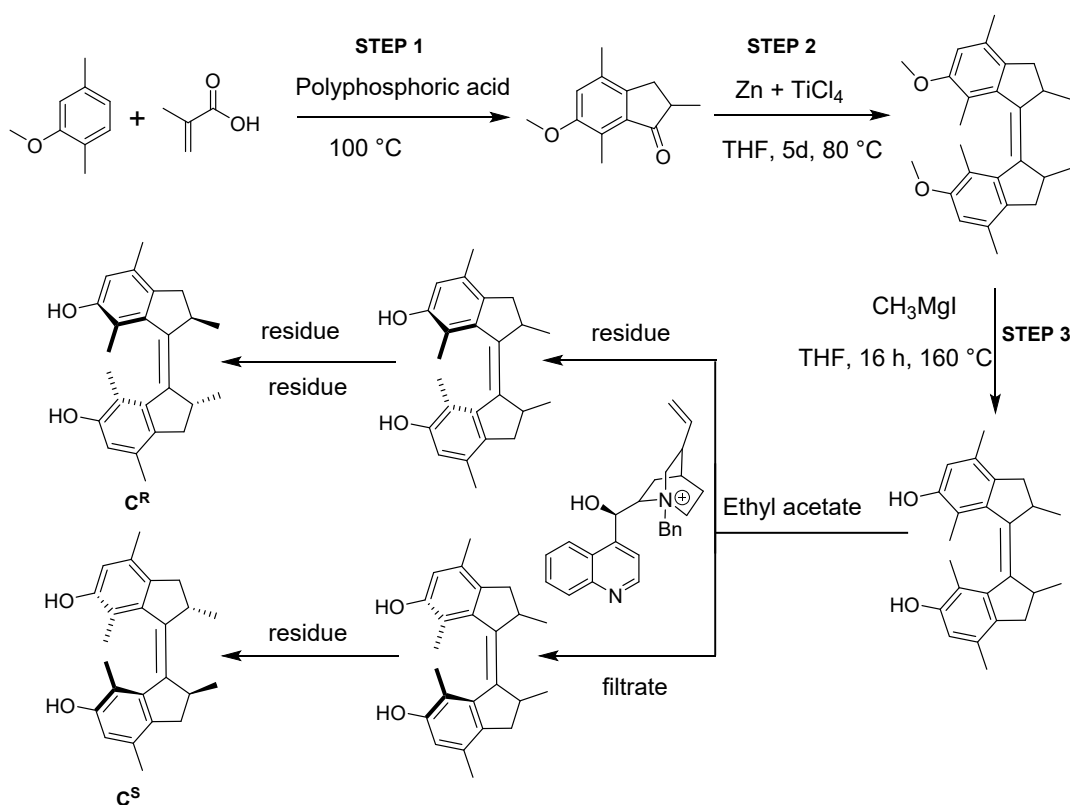
## ROP of Aib-NCA using chiral initiators (A\*, B\*, C\*) to prepare parent polymers

Polymers were synthesized using a previously published procedure<sup>2</sup>. In a typical procedure, a Schlenk tube equipped with a magnetic stirrer was subjected to 3 vacuum/N<sub>2</sub> cycles. Aib-NCA (0.200 g, 1.55 mmol, 1 eq) was added to the Schlenk tube and dissolved in dry DMF (~0.6 mL). The chiral initiator was added using an Eppendorf pipette for the amines or as solids for the binaphthol (B\*) and Feringa-type photoswitches (C\*) under a gentle counterflow of N<sub>2</sub> in an amount corresponding to the targeted monomer to initiator ratio: [M]/[I] = 15:1 for the amine initiators (A\*), and [M]/[I] = 30:1 for the binaphthol and the photoswitch initiators (B\*, C\*). The mixture was stirred at 80°C for 24 hours. The polymer was purified via dialysis in acetone using dialysis tubing with a molecular weight cutoff of 1 kDa for 3 days, and concentrated under reduced pressure to afford the parent polymers as a white solid. MALDI-TOF MS was used to assess the purity and chain length distributions for all parent polymers.

## General Procedure for End-Group modifications of Poly(Aib)

In a typical procedure, a predried two-neck round-bottom flask (50 mL), equipped with a magnetic stir bar, septum, and gas-tap, was filled with the carboxylic acids and the coupling agent. The solids were introduced to a nitrogen atmosphere and dissolved in 5-6 mL of dry solvent. Immediately after the addition of the solvent, DIPEA was added to form the activated carboxylic acid species. After 15 minutes of activation time, the poly(Aib) polymer (~50 mg, 1 eq.) was allowed to react at room temperature or at an elevated temperature for several days. The product was purified via dialysis in acetone for several days and concentrated in vacuum to yield the product as a powder. For the coupling conditions, refer to Table 1 of the main text. MALDI-TOF MS was used to assess the purity and chain length distributions for all modified polymers.

Synthesis and Chiral Resolution of Feringa Photoswitches: (2R, 2'R, Z)-2,2',4,4',7,7'-hexamethyl-2,2',3,3'-tetrahydro-[1,1'-biindenylidene]-6,6'-diol ( $C^R$ ) and (2S, 2'S, Z)-2,2',4,4',7,7'-hexamethyl-2,2',3,3'-tetrahydro-[1,1'-biindenylidene]-6,6'-diol ( $C^S$ ):

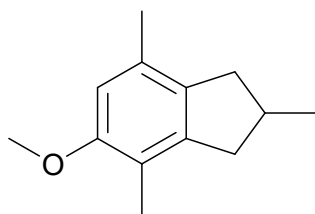


SI 2: Synthesis of second-generation Feringa-type overcrowded alkene photoswitch (diol) initiators ( $C^R$  and  $C^S$ ); three-step synthetic route and solvent-switchable chiral resolution with *N*-benzylcinchonidinium chloride

The photoswitches ( $C^R$  and  $C^S$ ) were synthesized using a previously used procedure<sup>3</sup>. The synthesis involved three steps and chiral resolution by a resolving agent.

### Step 1: Synthesis of 6-methoxy-2,4,7-trimethyl-2,3-dihydro-1H-inden-1-one

A mechanically stirred solution of 2,5-dimethylanisole (73.4 mmol, 1.0 eq, 10.36 mL) and methacrylic acid (146.85 mmol, 2.0 eq, 12.46 mL) in 200 g of polyphosphoric acid (105 %) was heated at 100 °C for 18 hours. The reaction mixture was quenched with ice and extracted with Diethyl Ether (Et<sub>2</sub>O) three times, each time using 400 mL. The organic layer was washed with a saturated aqueous solution of NaHCO<sub>3</sub> (400 mL) and a 1 M solution of NaOH (500 mL), and then dried over Na<sub>2</sub>SO<sub>4</sub>. The solvent was evaporated, and the crude product was purified by flash column chromatography (Hexane: Et<sub>2</sub>O = 95:5). The product was isolated as white crystals (58.9 % yield).

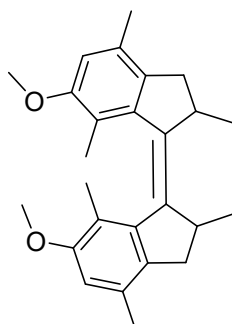


$^1\text{H}$  NMR (400 MHz,  $\text{cdCl}_3$ )  $\delta$  6.92 (s, 1H), 3.84 (s, 3H), 3.16 (dd,  $J = 16.7, 8.0$  Hz, 1H), 2.66 (m,  $J = 7.5, 4.1$  Hz, 1H), 2.50 (s, 3H), 2.46 (dd,  $J = 16.7, 4.1$  Hz, 1H), 2.29 (s, 3H), 1.29 (d,  $J = 7.4$  Hz, 3H)

$^{13}\text{C}$ -NMR (101 MHz,  $\text{cdCl}_3$ )  $\delta$  211.28, 157.10, 144.57, 134.33, 132.86, 124.27, 117.99, 56.50, 42.95, 32.61, 18.04, 16.70, 9.82 ppm.

## Step 2: Synthesis of 6,6'-dimethoxy-2,2',4,4',7,7'-hexamethyl-2,2',3,3'-tetrahydro-1,1'-biindenylidene

To a suspension of Zn powder (1.27 g, 19.56 mmol, 4 eq) in 10 mL anhydrous THF under a nitrogen atmosphere,  $\text{TiCl}_4$  (1.07 mL, 9.78 mmol, 2 eq) was slowly added via a syringe. The reaction mixture was heated at reflux for 2 hours, after which a solution of 6-methoxy-2,4,7-trimethyl-2,3-dihydro-1H-inden-1-one (1.0 g, 4.89 mmol, 1 eq) in THF (30 mL) was added via syringe. The mixture was heated at reflux for 5 days. The reaction mixture was poured into an aqueous solution of HCl (1 M, 40 mL) and extracted with EtOAc ( $2 \times 50$  mL). The organic layer was washed with a saturated aqueous solution of  $\text{NaHCO}_3$  (30 mL) and Brine (30 mL). The organic layer was dried over  $\text{Na}_2\text{SO}_4$ , and the solvent was dried under reduced pressure. Flash column chromatography (Hexane:  $\text{Et}_2\text{O} = 95:5$ ) yielded a white foamy crystalline solid (44.53 % yield).

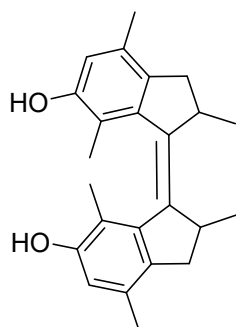


$^1\text{H}$ -NMR (402 MHz,  $\text{cdCl}_3$ )  $\delta$  6.57 (s, 2H), 3.87 (s, 6H), 2.97 – 2.85 (m, 2H), 2.61 (dd,  $J = 14.1, 5.7$  Hz, 2H), 2.31 (s, 6H), 2.21 (s, 6H), 2.17 (d,  $J = 14.1$  Hz, 2H), 1.10 (d,  $J = 6.5$  Hz, 6H) ppm.

$^{13}\text{C}$ -NMR (101 MHz,  $\text{cdCl}_3$ )  $\delta$  156.79, 142.45, 141.66, 133.97, 131.23, 120.21, 109.83, 55.68, 42.18, 38.34, 19.16, 18.66, 16.09 ppm.

### Step 3: Synthesis of 2,2',4,4',7,7'-hexamethyl-2,2',3,3'-tetrahydro-[1,1'-biindenylidene]-6,6'-diol

The alkene obtained from step 2 (2.80 mmol, 1.0 eq) was dissolved in dry THF and treated with  $\text{CH}_3\text{MgI}$  (16.8 mmol, 6.0 eq, 3M solution in  $\text{Et}_2\text{O}$ ) under a nitrogen atmosphere. The mixture was heated at  $160^\circ\text{C}$  for 16 h while allowing the solvent to evaporate slowly through a septum needle. After cooling, the reaction was quenched with ice and a saturated aqueous solution of  $\text{NH}_4\text{Cl}$ , followed by extraction with ethyl acetate ( $\text{EtOAc}$ ). The organic phase was washed with brine, dried, and concentrated. Purification was performed using flash column chromatography, which yielded the racemic diol as a white solid (62.7% yield).



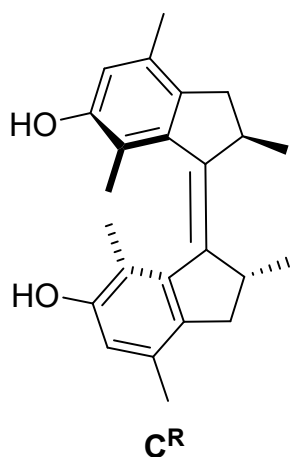
$^1\text{H}$ -NMR (402 MHz,  $\text{cd}_3\text{cn}$ )  $\delta$  6.50 (s, 2H), 6.32 (s, 2H), 3.33 (p,  $J = 6.7$  Hz, 2H), 2.99 (dd,  $J = 14.6, 6.3$  Hz, 2H), 2.39 (d,  $J = 14.6$  Hz, 2H), 2.18 (s, 6H), 1.32 (s, 6H), 1.03 (d,  $J = 6.8$  Hz, 6H) ppm.

$^{13}\text{C}$ -NMR (101 MHz,  $\text{cd}_3\text{cn}$ )  $\delta$  153.23, 142.14, 140.85, 135.51, 131.12, 119.35, 117.27, 114.49, 41.76, 37.66, 19.69, 17.47, 13.46 ppm.

### Optical Resolution

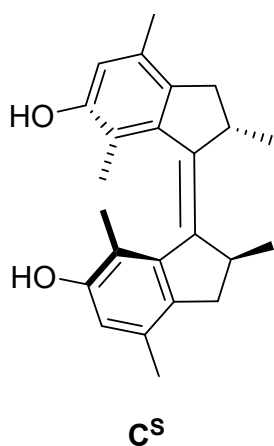
The racemic diol obtained in step 3 was subjected to chiral resolution using (8S,9R)-N-benzylcinchonidinium chloride as a resolving agent, following a modified literature procedure<sup>3</sup>. To a solution of the racemate in ethyl acetate, the resolving agent was added, and the mixture was stirred at room temperature under a nitrogen atmosphere for 16 h. The suspension was then filtered, and the solid and filtrate were processed separately. The filtrate was extracted with 1 M aqueous HCl, washed successively with a saturated  $\text{NaHCO}_3$  solution and brine, dried over  $\text{Na}_2\text{SO}_4$ , and concentrated under reduced pressure to yield one enantiomer as a pale brown solid. The solid residue collected on the filter was dissolved in methanol, concentrated, and re-extracted with ethyl acetate and 1 M HCl. The organic phase was washed with a saturated  $\text{NaHCO}_3$  solution and brine, dried over  $\text{Na}_2\text{SO}_4$ , and evaporated to yield the opposite enantiomer as a pale-yellow solid. Both materials were further purified by repeating the resolution under analogous conditions. The final products, (2R,2'R,Z)-2,2',4,4',7,7'-

hexamethyl-2,2',3,3'-tetrahydro-[1,1'-biindenylidene]-6,6'-diol, and (2*S*,2'*S*,*Z*)-2,2',4,4',7,7'-hexamethyl-2,2',3,3'-tetrahydro-[1,1'-biindenyl]-6,6'-diol, were obtained in the form of a pale-yellow solid in 44.2% and 33.9% recovery, respectively. Successful resolution was confirmed by CD spectroscopy, which displayed mirror-image spectra for the two enantiomers (see SI 54).



<sup>1</sup>H NMR (500 MHz, cd<sub>3</sub>cn) δ 6.50 (s, 2H), 6.32 (s, *J* = 1.2 Hz, 2H), 3.33 (p, *J* = 6.7 Hz, 2H), 2.99 (dd, *J* = 14.5, 6.3 Hz, 2H), 2.39 (d, *J* = 14.5 Hz, 2H), 2.19 – 2.17 (m, 6H), 2.16 (d, *J* = 0.8 Hz, 1H), 1.32 (s, 6H), 1.03 (d, *J* = 6.8 Hz, 6H).

<sup>13</sup>C NMR (126 MHz, cd<sub>3</sub>cn) δ 154.24, 143.15, 141.86, 136.52, 132.13, 120.36, 118.24, 115.51, 42.78, 38.68, 20.71, 18.49, 14.49, 1.63, 1.47, 1.36.

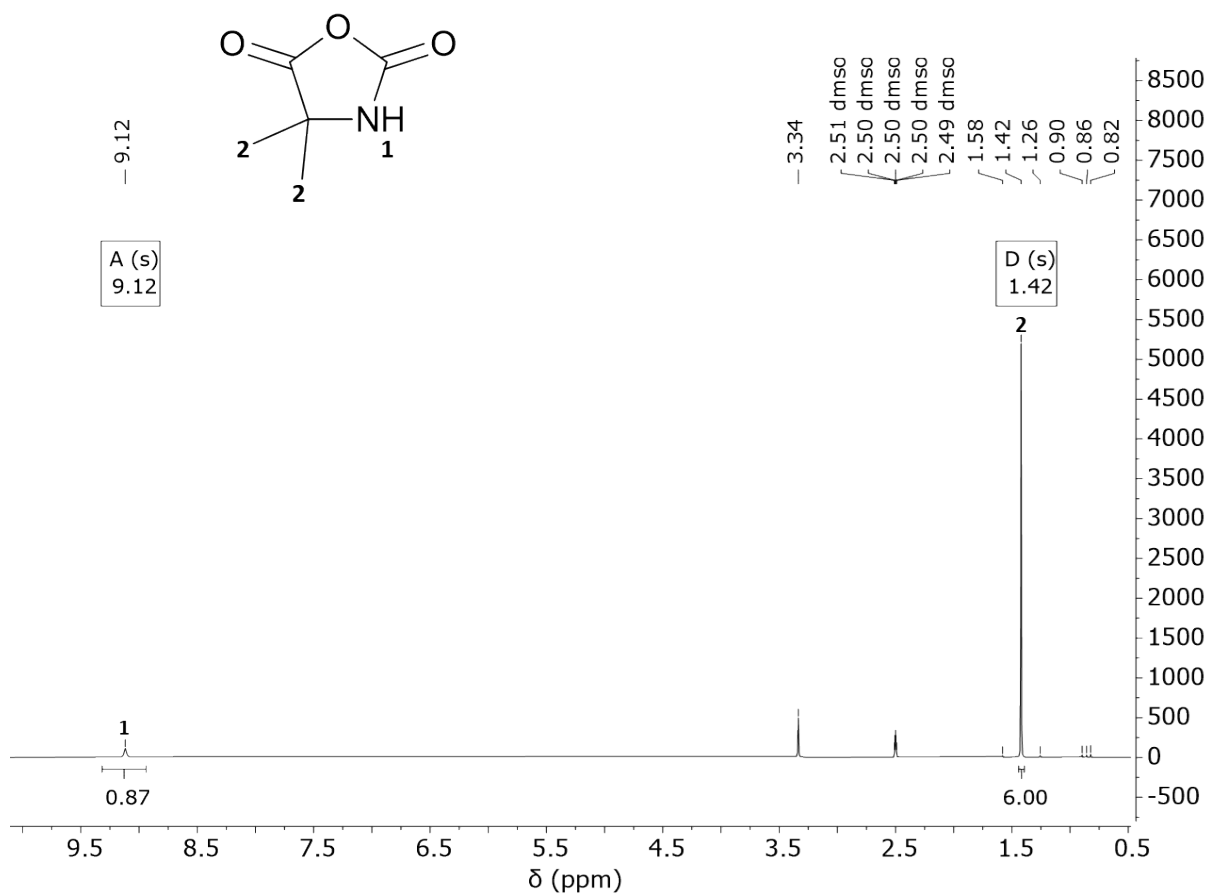


<sup>1</sup>H NMR (500 MHz, cd<sub>3</sub>cn) δ 6.54 (s, 2H), 6.36 (s, 2H), 3.36 (p, *J* = 6.7 Hz, 2H), 3.02 (dd, *J* = 14.6, 6.3 Hz, 2H), 2.42 (d, *J* = 14.6 Hz, 2H), 2.21 (s, 6H), 1.35 (s, 5H), 1.07 (d, *J* = 6.8 Hz, 6H).

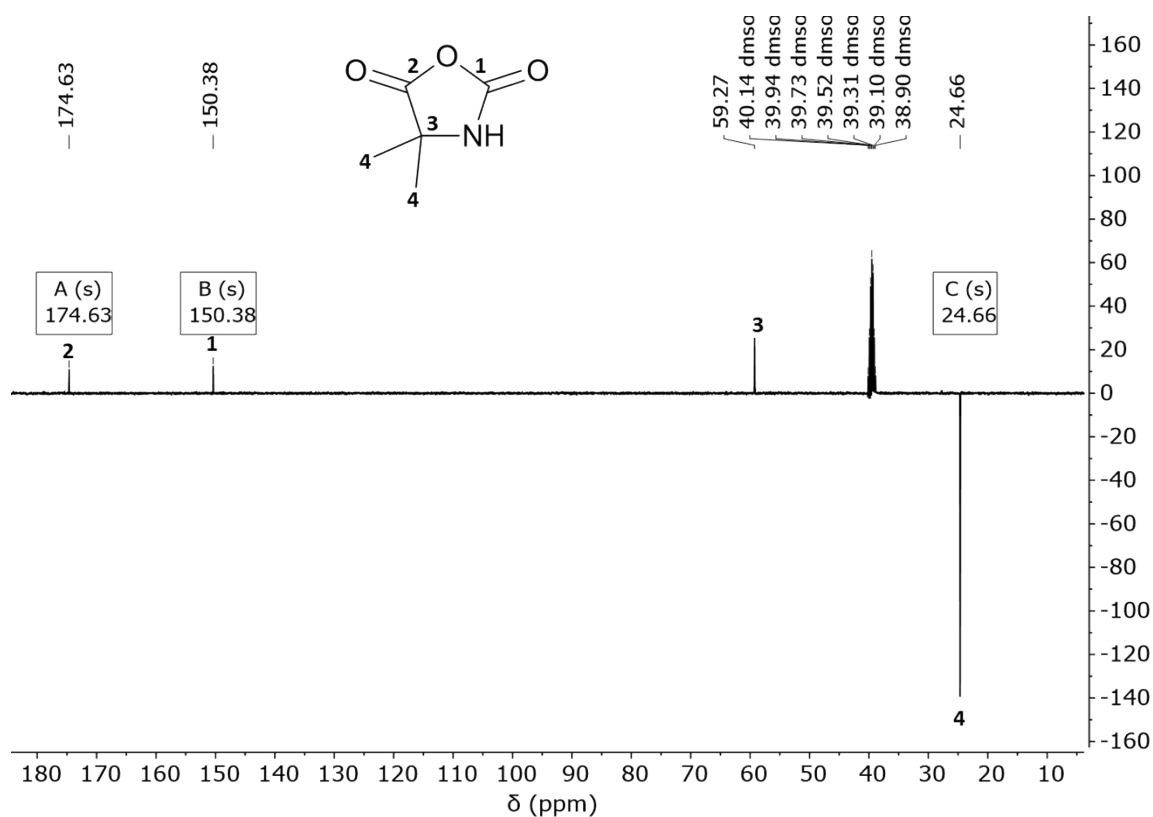
$^{13}\text{C}$  NMR (126 MHz,  $\text{cdCl}_3$ )  $\delta$  152.25, 142.19, 140.87, 136.46, 131.49, 118.55, 114.64, 77.24, 76.99, 76.74, 41.81, 38.10, 20.40, 18.42, 18.37, 13.67.

## NMR Analysis

### NMR Analysis of Aib-NCA monomer

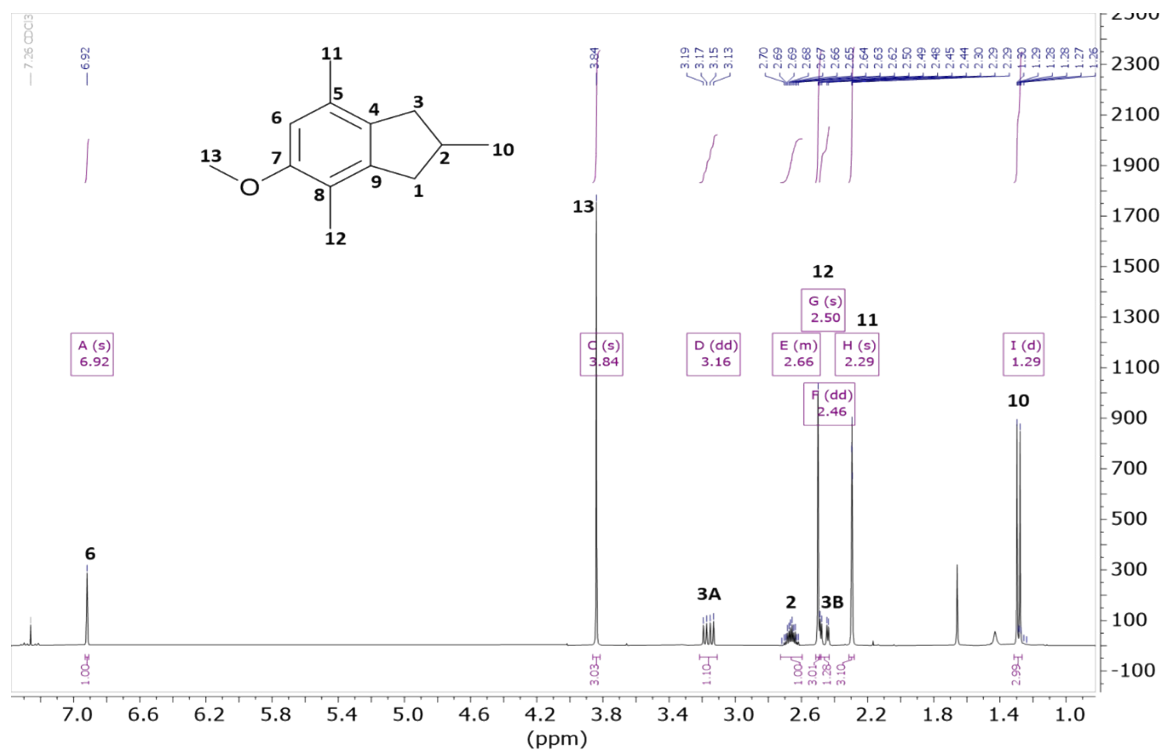


SI 3:  $^1\text{H}$ -NMR Spectrum (400 MHz,  $\text{DMSO-d}_6$ , 298 K) of Aib-NCA

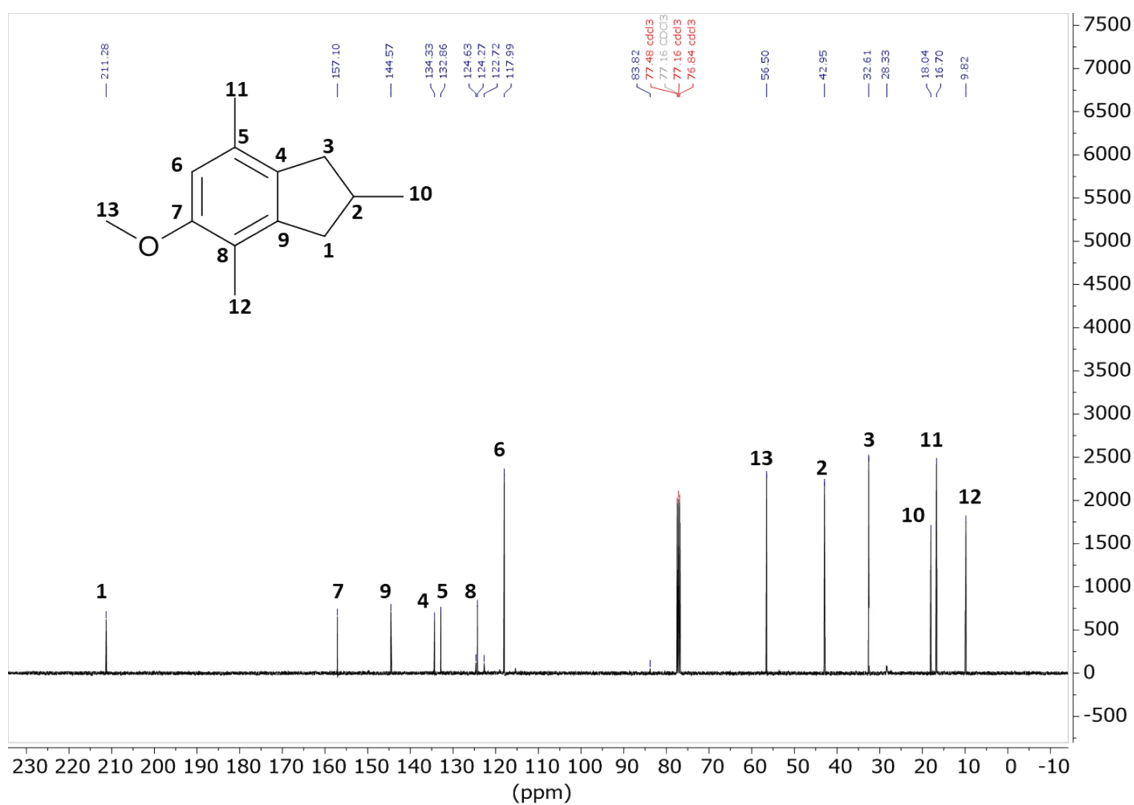


SI 4: APT (101 MHz, DMSO-*d*<sup>6</sup>, 298 K) of Aib-NCA

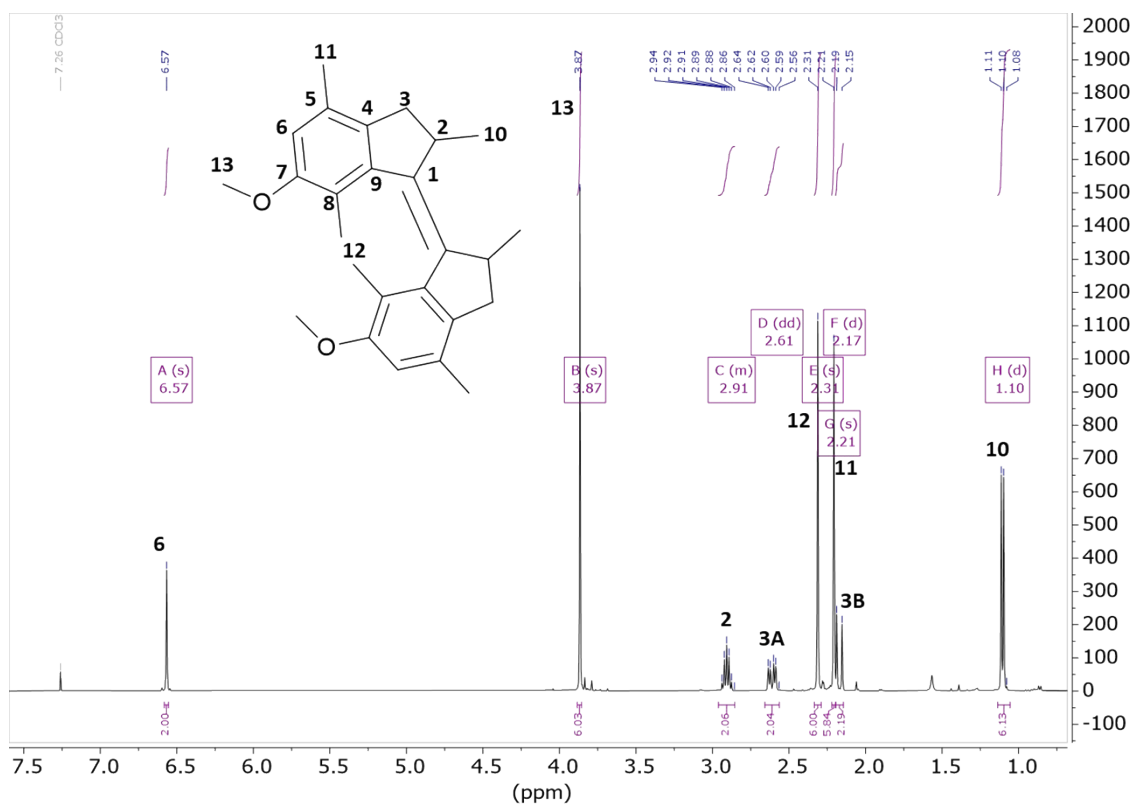
## Stepwise NMR Analysis of the Feringa Photoswitch Synthesis



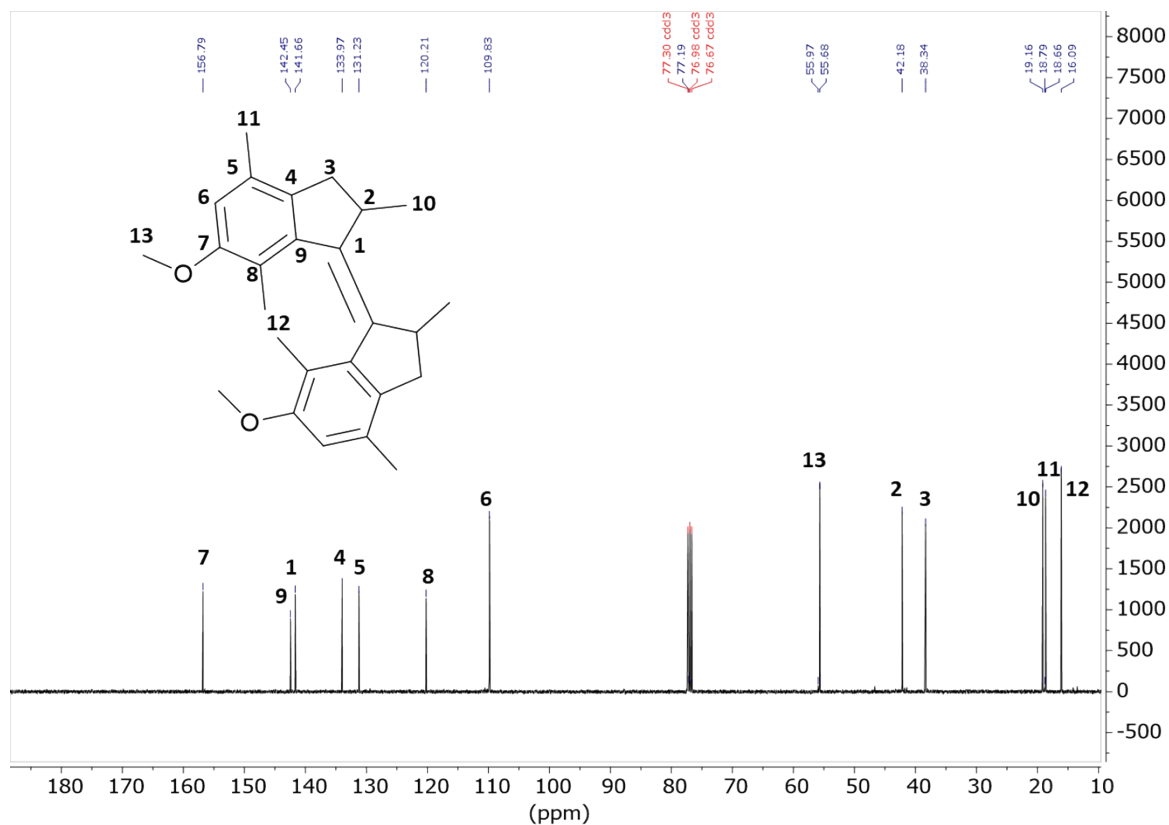
SI 5: <sup>1</sup>H-NMR Spectroscopy (400 MHz, CDCl<sub>3</sub>, 298K) of 6-methoxy-2,4,7-trimethyl-2,3-dihydro-1H-inden-1-one (Step 1)



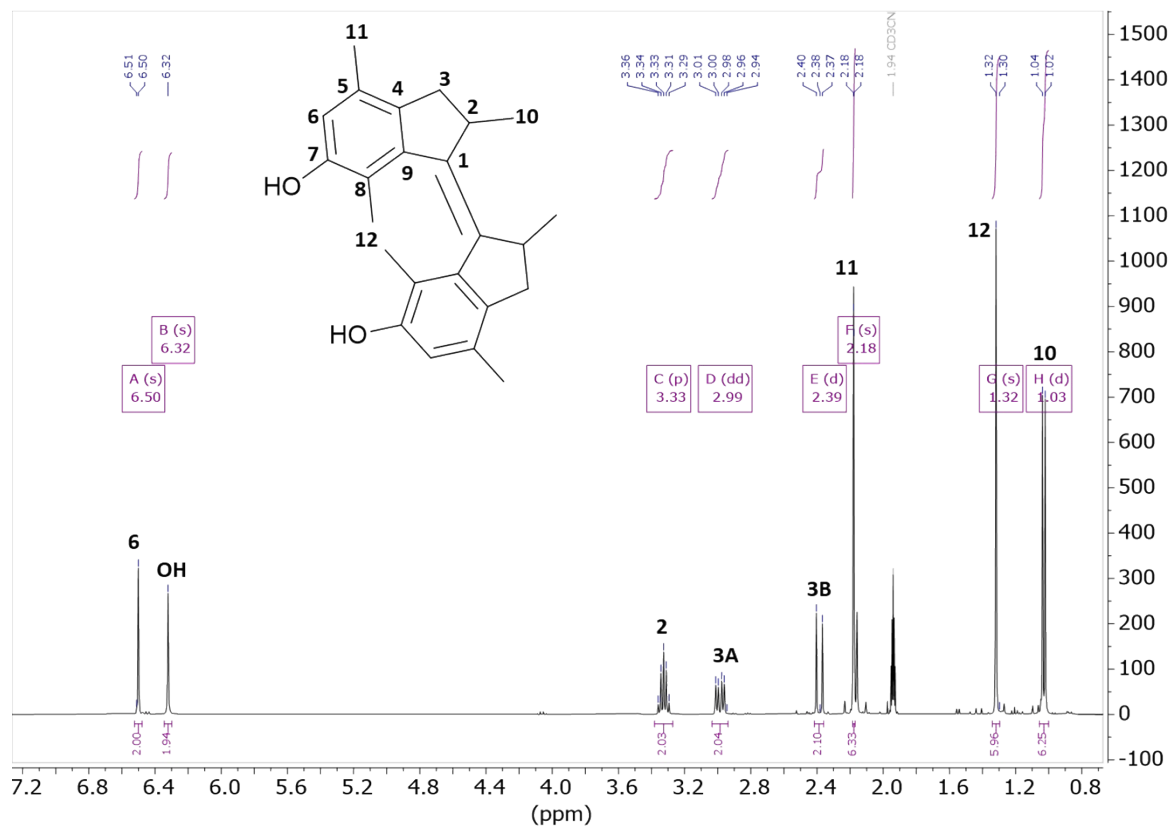
SI 6: <sup>13</sup>C-NMR Spectroscopy (101 MHz, CDCl<sub>3</sub>, 298K) of 6-methoxy-2,4,7-trimethyl-2,3-dihydro-1H-inden-1-one (Step 1)



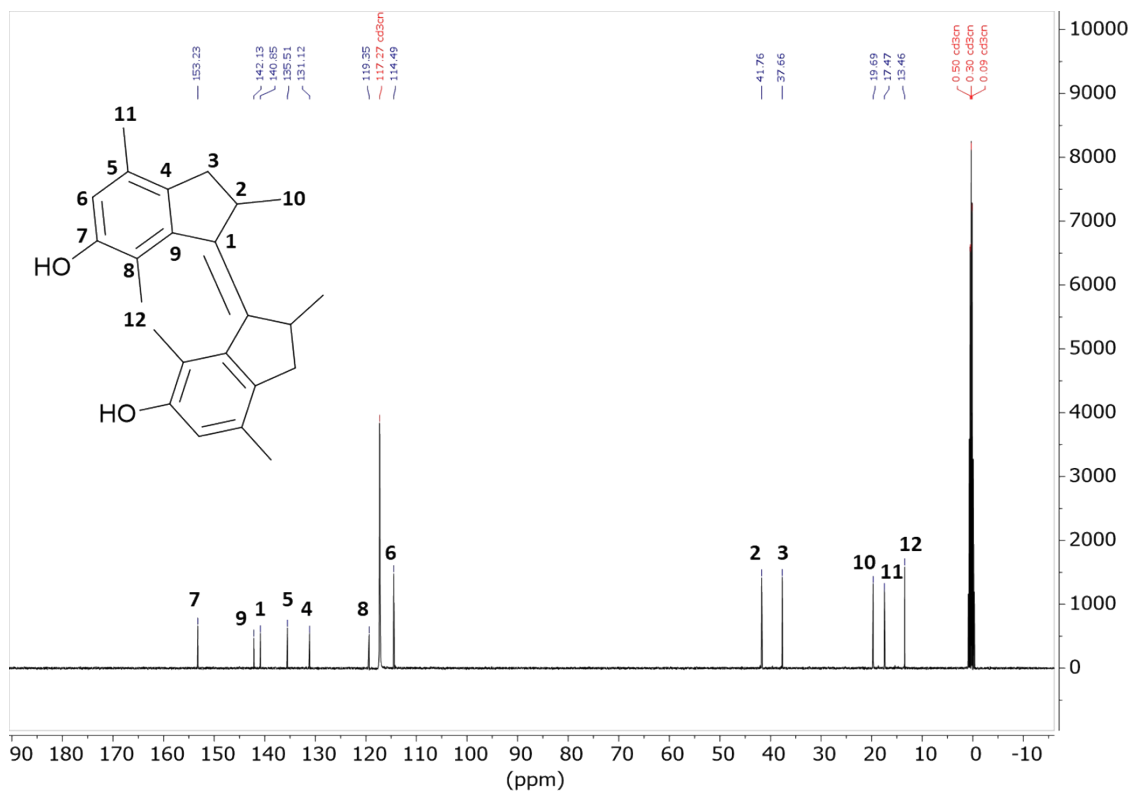
SI 7: <sup>1</sup>H-NMR Spectroscopy (402 MHz, CDCl<sub>3</sub>, 298K) of 6,6'-dimethoxy-2,2',4,4',7,7'-hexamethyl-2,2',3,3'-tetrahydro-1,1'-biindenylidene (Step 2)



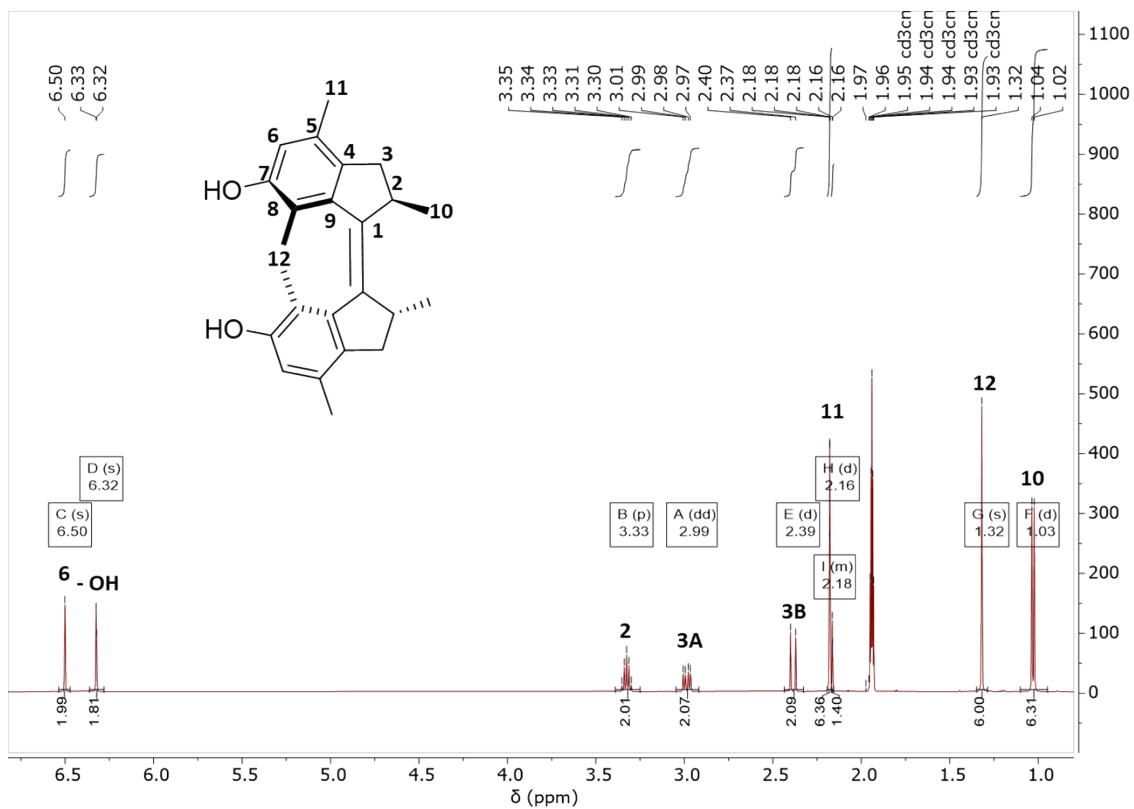
SI 8: <sup>13</sup>C-NMR Spectroscopy (101 MHz, CDCl<sub>3</sub>, 298K) of 6,6'-dimethoxy-2,2',4,4',7,7'-hexamethyl-2,2',3,3'-tetrahydro-1,1'-biindenylidene (Step 2)



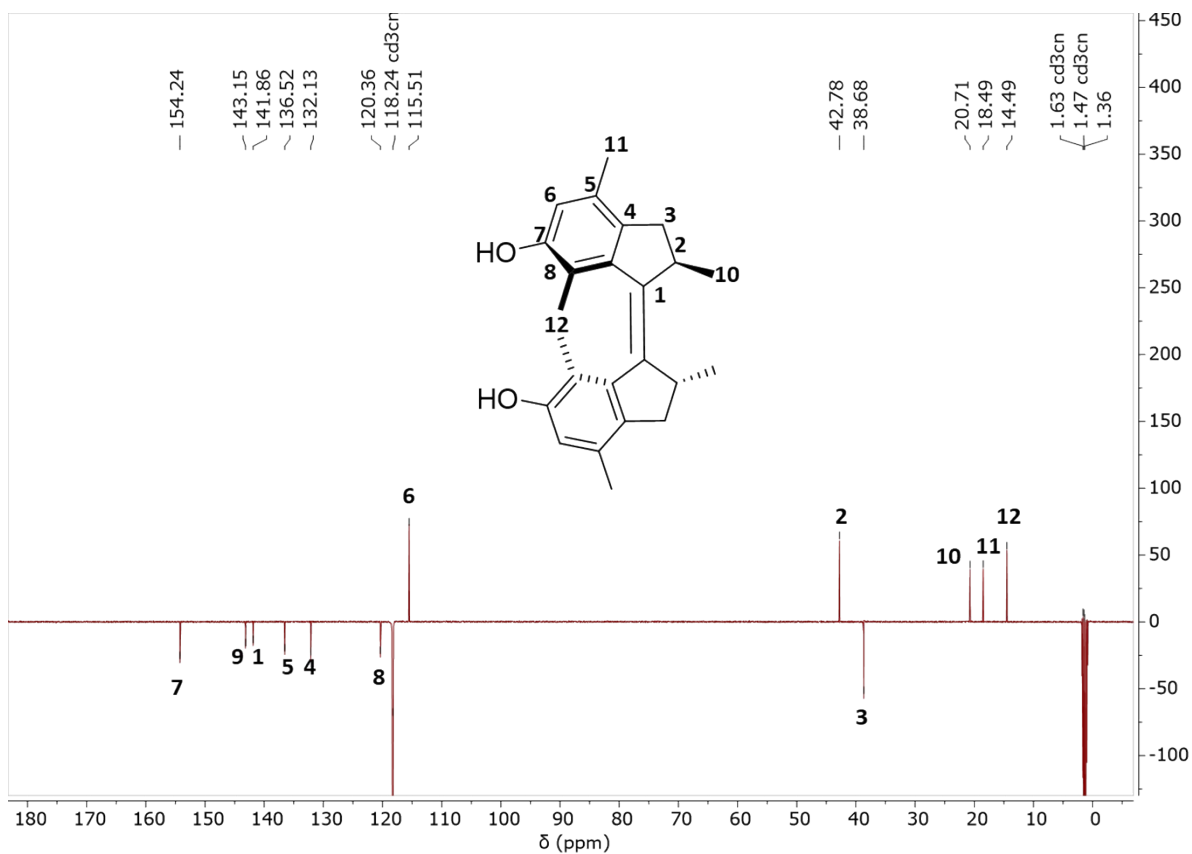
SI 9: <sup>1</sup>H-NMR Spectroscopy (402 MHz, CD<sub>3</sub>CN, 298K) of 2,2',4,4',7,7'-hexamethyl-2,2',3,3'-tetrahydro-[1,1'-biindenylidene]-6,6'-diol (Step 3)



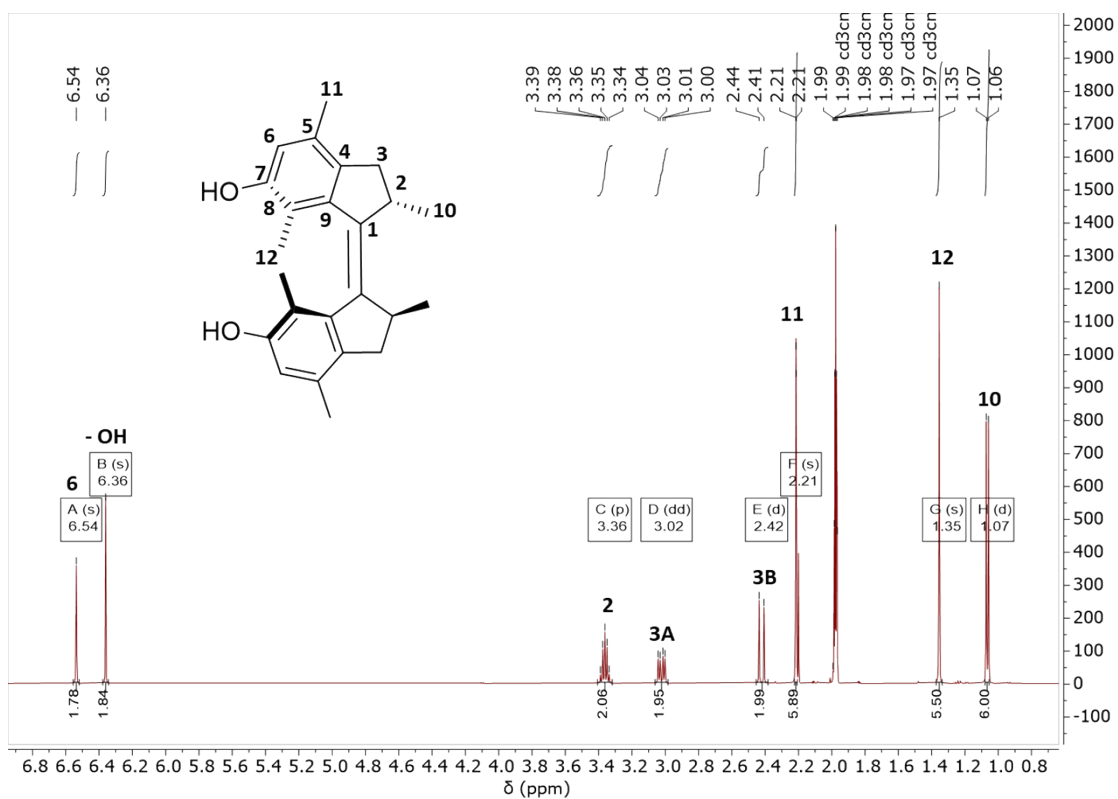
SI 10:  $^{13}\text{C}$ -NMR Spectroscopy (101 MHz,  $\text{CD}_3\text{CN}$ , 298K) of 2,2',4,4',7,7'-hexamethyl-2,2',3,3'-tetrahydro-[1,1'-biindenylidene]-6,6'-diol (Step 3)



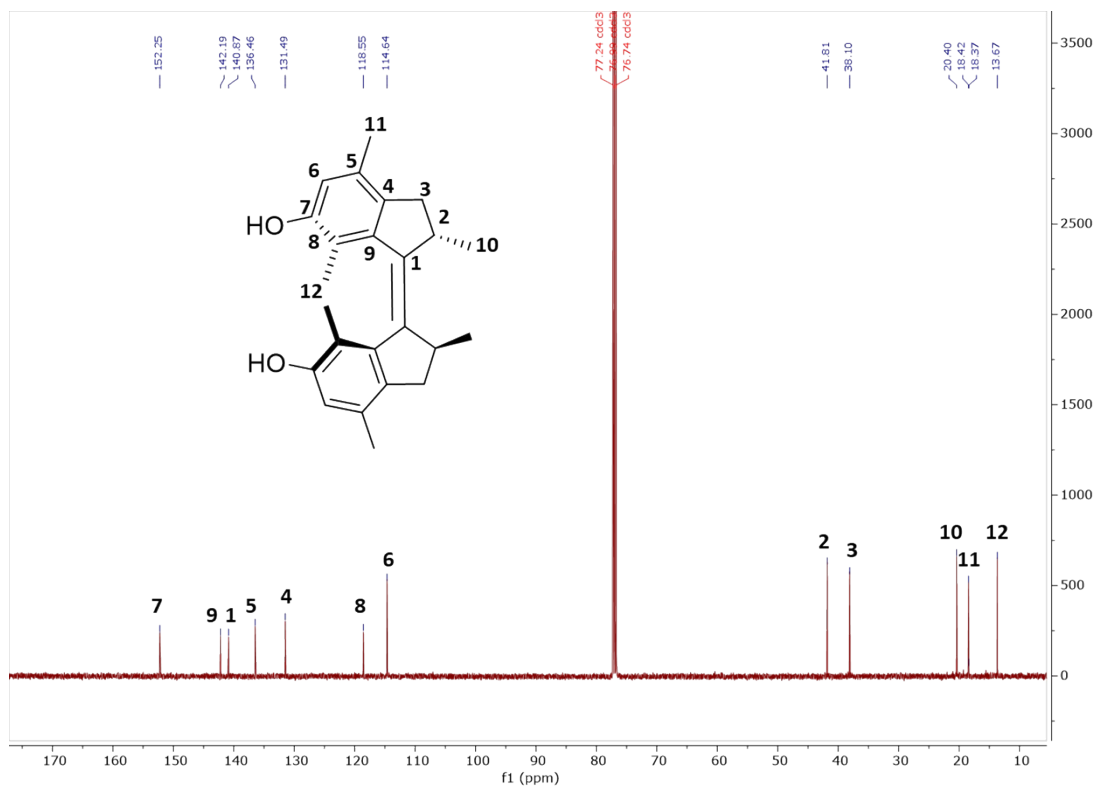
SI 11:  $^1\text{H}$ -NMR Spectroscopy (500 MHz,  $\text{CD}_3\text{CN}$ , 298K) of (2R,2'R,Z)-2,2',4,4',7,7'-hexamethyl-2,2',3,3'-tetrahydro-[1,1'-biindenylidene]-6,6'-diol ( $\text{C}^R$ )



SI 12:  $^{13}C$ -NMR Spectroscopy (126 MHz,  $CD_3CN$ , 298K) of (2R,2'R,Z)-2,2',4,4',7,7'-hexamethyl-2,2',3,3'-tetrahydro-[1,1'-biindenylidene]-6,6'-diol ( $C^R$ )

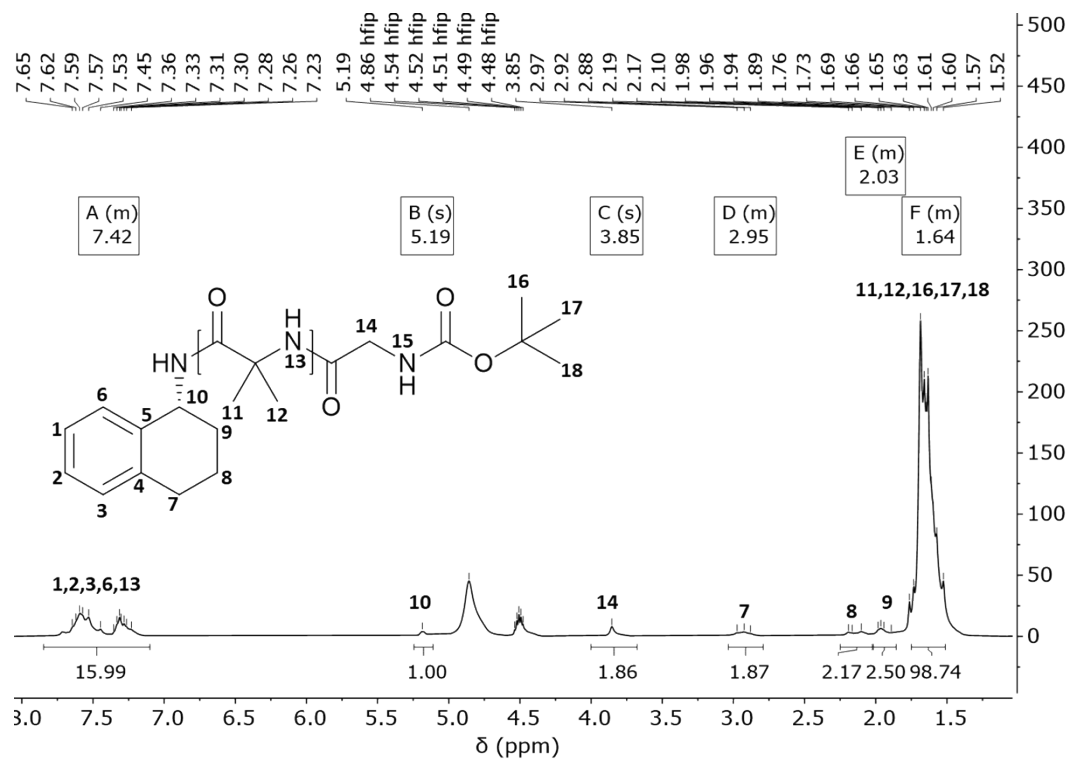


SI 13:  $^1H$ -NMR Spectroscopy (500 MHz,  $CD_3CN$ , 298K) of (2S,2'S,Z)-2,2',4,4',7,7'-hexamethyl-2,2',3,3'-tetrahydro-[1,1'-biindenylidene]-6,6'-diol ( $C^S$ )



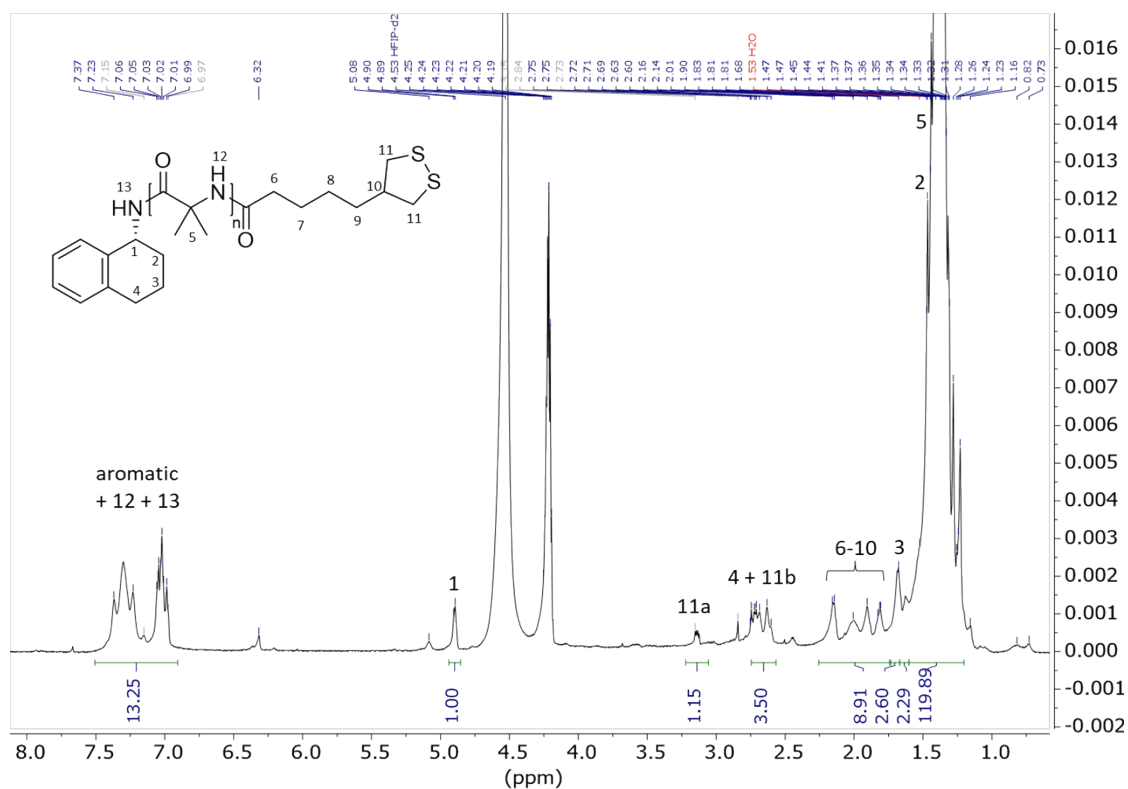
SI 14:  $^{13}\text{C}$ -NMR Spectroscopy (126 MHz,  $\text{CDCl}_3$ , 298K) of (2S,2'S, Z)-2,2',4,4',7,7'-hexamethyl-2,2',3,3'-tetrahydro-[1,1'-biiindenylidene]-6,6'-diol ( $\text{C}^5$ )

## NMR Analysis of End-Group Modified Polymers



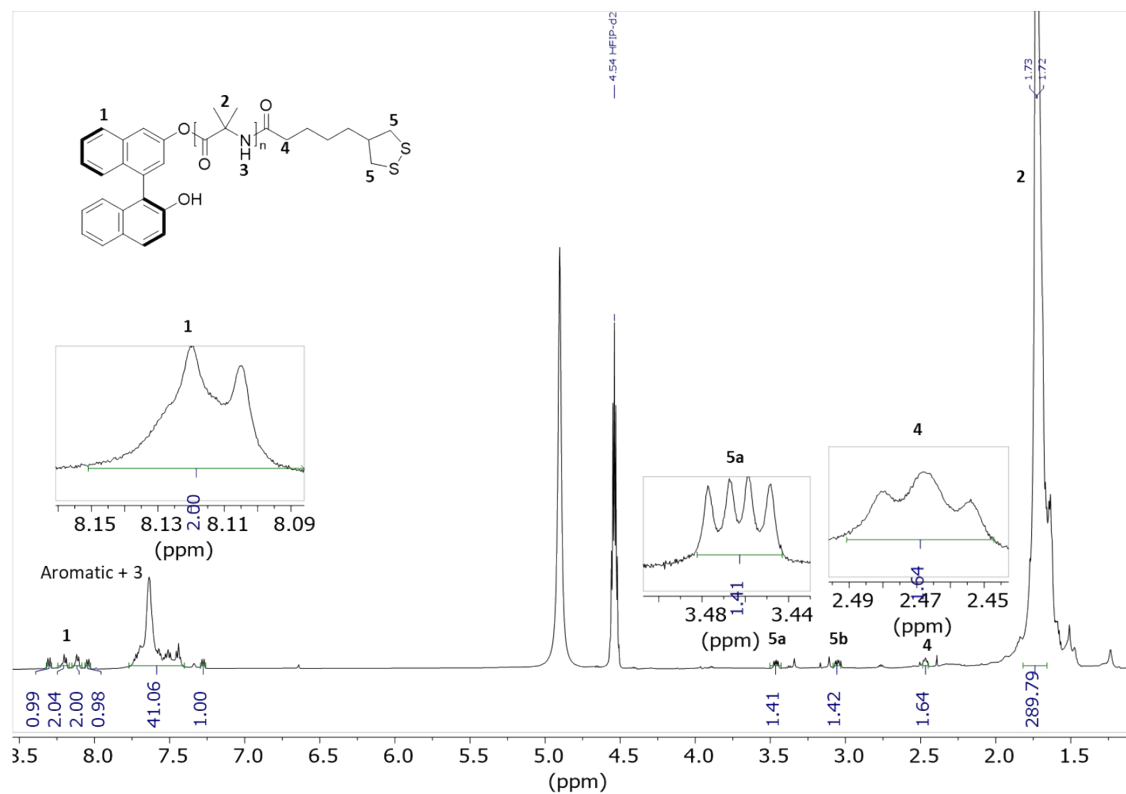
SI 15:  $^1\text{H}$ -NMR Spectroscopy (402 MHz, HFIP, 298K) of  $\text{A}^{\text{R}}\text{-P}_4\text{-E}_3$  (Signal 10 used as reference)

Approximate End-Group Conversion: The conversion was estimated from the end-group signal (peak 14), which is expected to integrate to 2H for complete modification. The observed integral was 1.86 H, corresponding to  $(1.86/2) \times 100 = 93\%$  conversion.



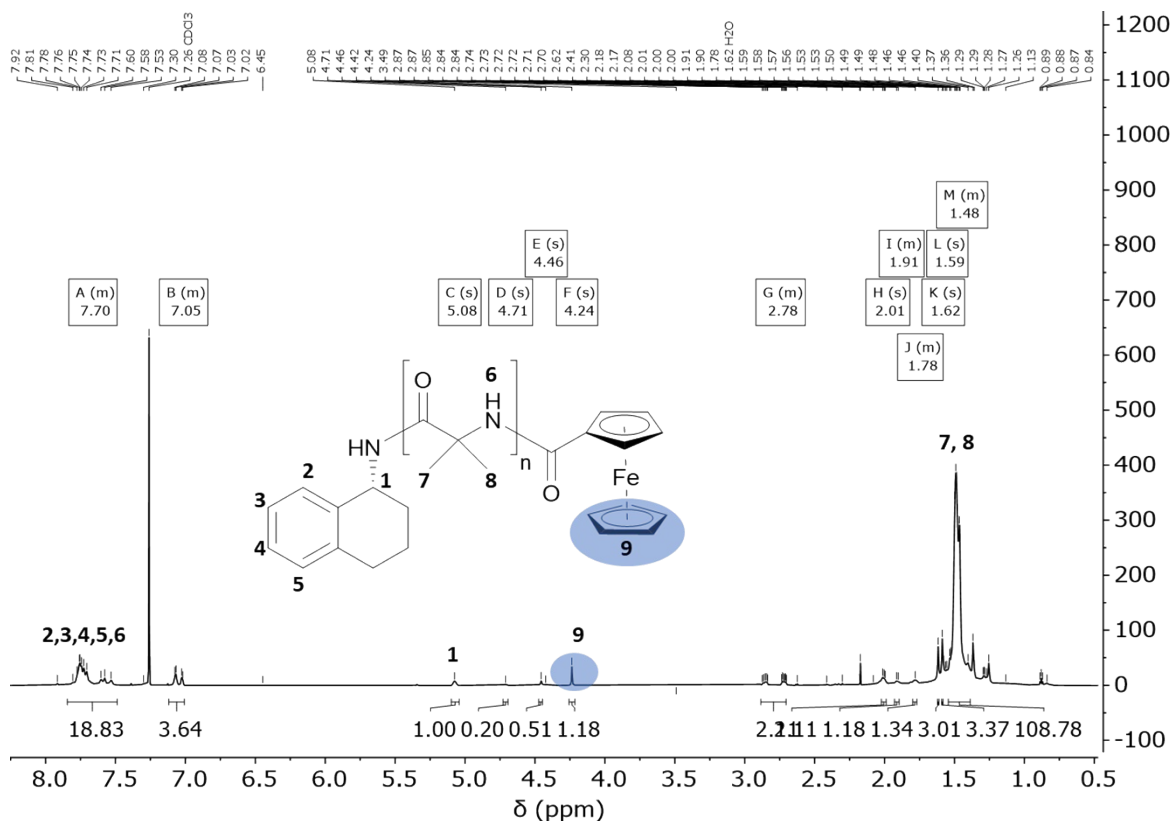
SI 16: <sup>1</sup>H-NMR Spectroscopy (600 MHz, HFIP, 298K) of *A<sup>R</sup>-P<sub>8</sub>-E<sub>1</sub>* (Signal 1 used as reference)

Approximate End-Group Conversion: The conversion was estimated from the end-group signal (peak 11a), which is expected to integrate to 2H for complete modification. The observed integral was 1.15 H, corresponding to  $(1.15/2) \times 100 = 57.5\%$  conversion.



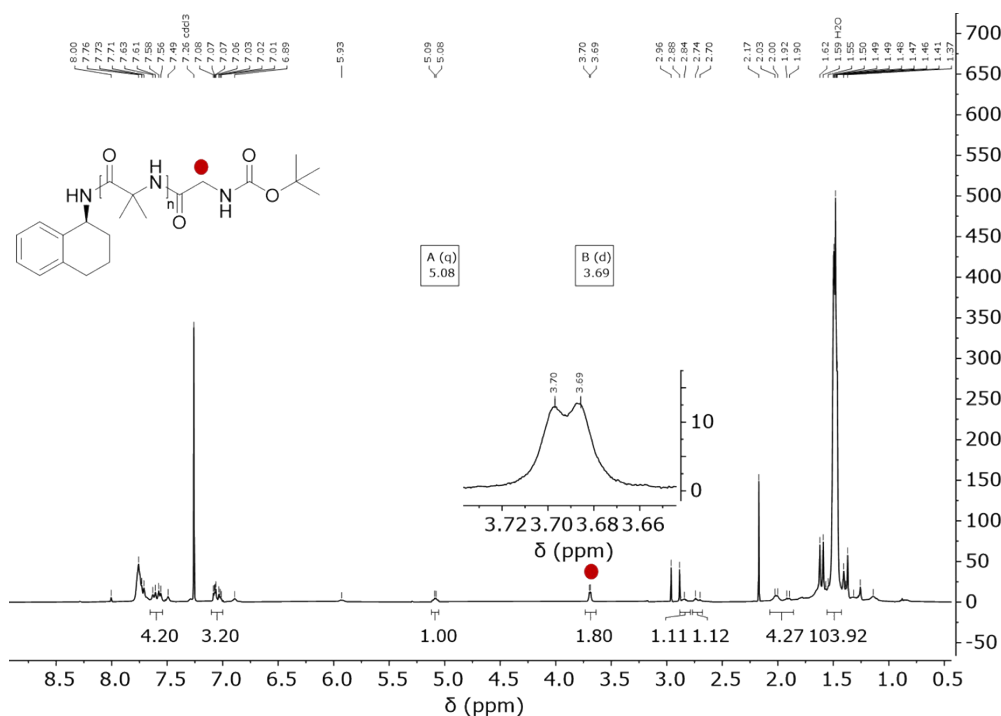
SI 17  $^1H$ -NMR Spectroscopy (800 MHz,  $CDCl_3$ , 298K) of  $B^5-P_{14}-E_1$  (Signal 1 used as reference)

Approximate End-Group Conversion: The conversion was estimated from the end-group signal (peak 5a), which is expected to integrate to 2H for complete modification. The observed integral was 1.41 H, corresponding to  $(1.15/2) \times 100 = 70.5\%$  conversion



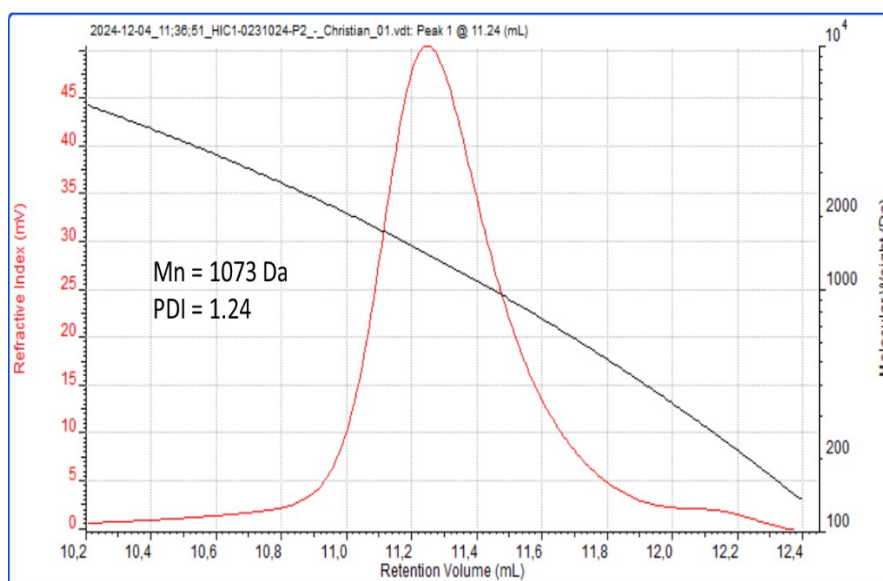
SI 18  $^1\text{H-NMR}$  Spectroscopy (800 MHz,  $\text{CDCl}_3$ , 298K) of  $A^5-P_7-E_4$  (Signal 1 used as reference)

Approximate End-Group Conversion: The conversion was estimated from the end-group signal (peak 9), which is expected to integrate to 5H from the protons of the Cp ring for complete modification. The observed integral was 1.15 H, corresponding to  $(1.18/5) \times 100 = 23.6\%$  conversion.



SI 19  $^1\text{H-NMR}$  spectra of Boc-Gly functionalized poly(Aib) derivative  $A^4-P_4-E_3$  in  $\text{CDCl}_3$

## GPC Analysis



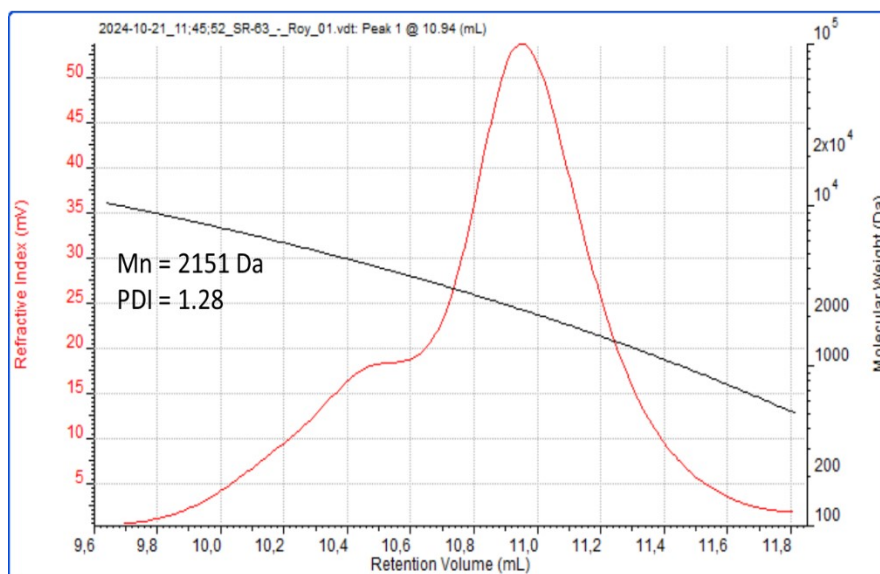
Conventional Calibration - Homopolymers results

Peak	1
Ret Vol (mL)	11.242
Mn (Da)	1.073
Mw (Da)	1.337
Mz (Da)	1.624
Mp (Da)	1.381
Mw/Mn	1.246
% Above 0	100.0000
% Below 0	0.0000
Wt Fr (Peak)	1.0000
RI Area (mV/mL)	23.69
UV Area (mV/mL)	0.00

Run conditions

Method File	PMMA_conv_0_6-62 21Da_05 09-0007.vcm
Solvent	HFP + KTFAC 0.1mol/l
Date Acquired	Dec 04, 2024 - 11:38:51
Acquisition Operator	admin : Administrator
Calculation Operator	admin : Administrator
Column Set	PSS PFG Vor-Trennsäule
System	GPC-3
Flow Rate (ml/min)	0.5000
Injection Volume (ul)	100.0
Volume Increment	0.0083
Detector Temp (C)	35.00
Column Temp (C)	22.00
OmnISEC Version	467

SI 20: GPC measurements of  $A^R-P_0-E_0$  with the corresponding molecular weights and polydispersity index (PDI).



Conventional Calibration - Homopolymers results

Peak	1
Ret Vol (mL)	10.942
Mn (Da)	2.151
Mw (Da)	2.762
Mz (Da)	3.540
Mp (Da)	2.212
Mw/Mn	1.284
% Above 0	100.0000
% Below 0	0.0000
Wt Fr (Peak)	1.0000
RI Area (mV.mL)	35.55
UV Area (mV.mL)	0.00

Run conditions

Method File	PMMA_conv_0.6-62.2kDa_05.09-0007.vcm
Solvent	HFP + KTFAC 0.1mol/l
Date Acquired	Oct 21, 2024 - 11:45:52
Acquisition Operator	admin : Administrator
Calculation Operator	admin : Administrator
Column Set	PSS PFG Var-Trennsäule
System	GPC-3
Flow Rate (ml/min)	0.5000
Injection Volume (ul)	100.0
Volume Increment	0.0083
Detector Temp (C)	35.00
Column Temp (C)	22.00
OmniSEC Version	467

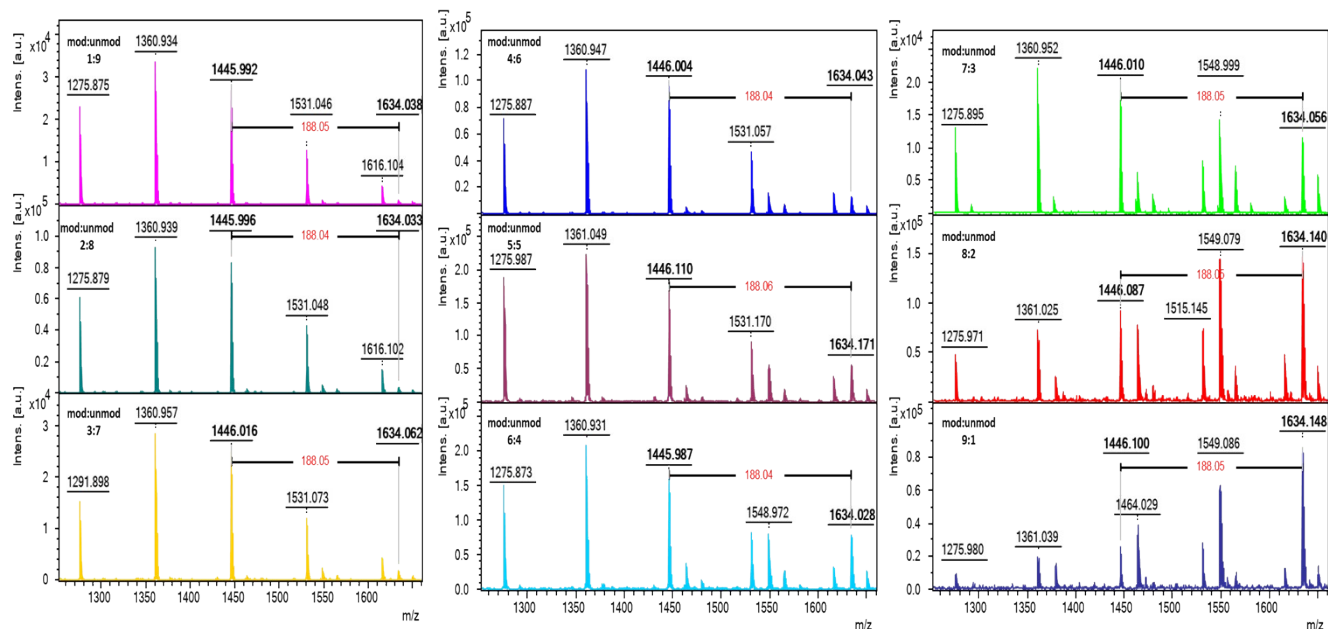
SI 21: GPC measurements of  $B^R-P_0-E_0$  with the corresponding molecular weights and polydispersity index (PDI).

## MALDI-TOF Analysis

### Sensitivity Analysis

The influence of end-group identity on MALDI signal intensity was evaluated using sensitivity plots, as described in the literature. Mixtures of a liponic-acid-modified sample ( $A^R-P_{11}-E_2$ ; “mod”) and its unmodified parent ( $A^R-P_0-E_0$ ) were prepared at defined mass ratios  $W_{\text{mod}}/W_{\text{unmod}} = 0.11, 0.25, 0.43, 0.67, 1.0, 1.5, 2.33, 4.0, 9.0$  by combining 20 mg mL<sup>-1</sup> DMF stock solutions of the two polymers (1-9  $\mu$ L of “mod” with 9-1  $\mu$ L of “unmod”), together with matrix and salt (dithranol and NaTFA; final matrix: analyte: salt = 100: 10: 1; 1  $\mu$ L spotted). All spectra were acquired with a laser power of 32%, an accelerating voltage of 19.43 kV, and the instrument’s medium laser spot. The MALDI spectra of the nine mixtures are shown in SI 20. Peak intensities of Na<sup>+</sup> adducts at identical chain lengths (DP = 15) were measured for the modified and unmodified series, giving  $I_{\text{mod}}$  and  $I_{\text{unmod}}$ , respectively. The ratio of  $I_{\text{mod}}/I_{\text{unmod}}$  was plotted versus the mixing mass ratio  $W_{\text{mod}}/W_{\text{unmod}}$  (SI 21), yielding a linear correlation ( $R^2 \approx 0.992$ ,  $r \approx 0.996$ ). This calibration was performed only to verify that modified and unmodified chains exhibit a predictable, linear intensity response under identical conditions; no response factor was applied to other datasets acquired under different parameters. End-group conversion

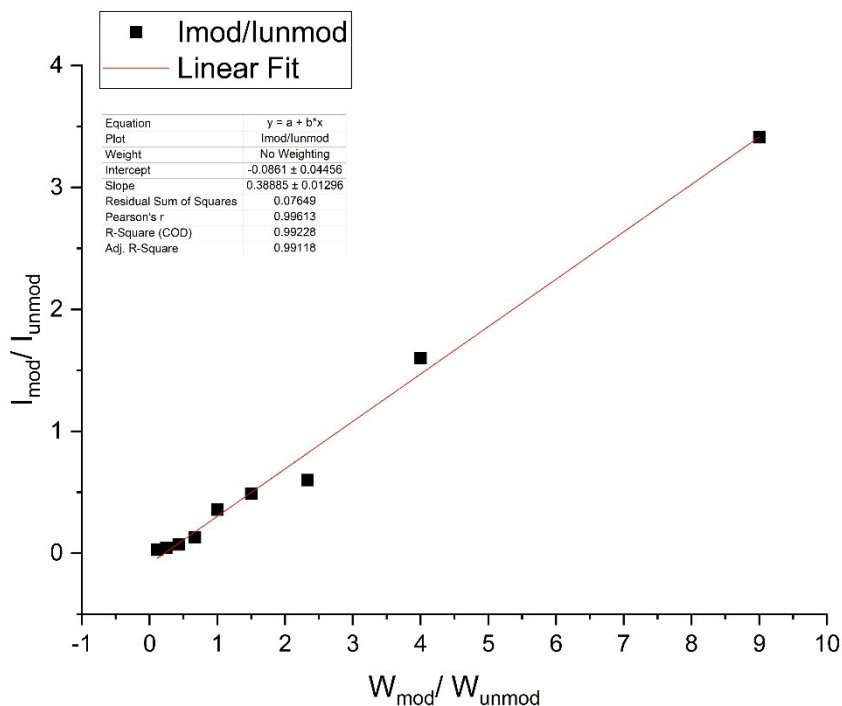
(%) was quantified from MALDI-TOF MS by comparing the signal intensity of the modified chains to the sum of the modified and unmodified chains at the same degree of polymerization (DP) and the same alkali adduct.



SI 22: MALDI-TOF MS spectra of the samples for  $A^R-P_{11}-E_2/A^R-P_0-E_0$  mixtures

Table 1: Mixture compositions and corresponding MALDI  $I_{mod}/I_{unmod}$  ratios

$W_{mod}/W_{unmod}$	Mod ( $\mu\text{L}$ )	Unmod ( $\mu\text{L}$ )	Matrix ( $\mu\text{L}$ )	Salt ( $\mu\text{L}$ )	$I_{mod}$	$I_{unmod}$	$I_{mod}/I_{unmod}$
0.11	1	9	100	1	764	27773	0.028
0.25	2	8	100	1	3717	85622	0.043
0.43	3	7	100	1	1782	25314	0.070
0.67	4	6	100	1	12733	96922	0.131
1.0	5	5	100	1	61286	171745	0.356
1.5	6	4	100	1	82122	168195	0.488
2.33	7	3	100	1	11973	19876	0.6
4.0	8	2	100	1	150206	90148	1.6
9.0	9	1	100	1	89199	26083	3.41



SI 23: Plot of total signal intensity ratios vs. weight ratios of  $A^R-P_{11}-E_2$  and  $A^R-P_0-E_0$

## End-group Conversion Calculation

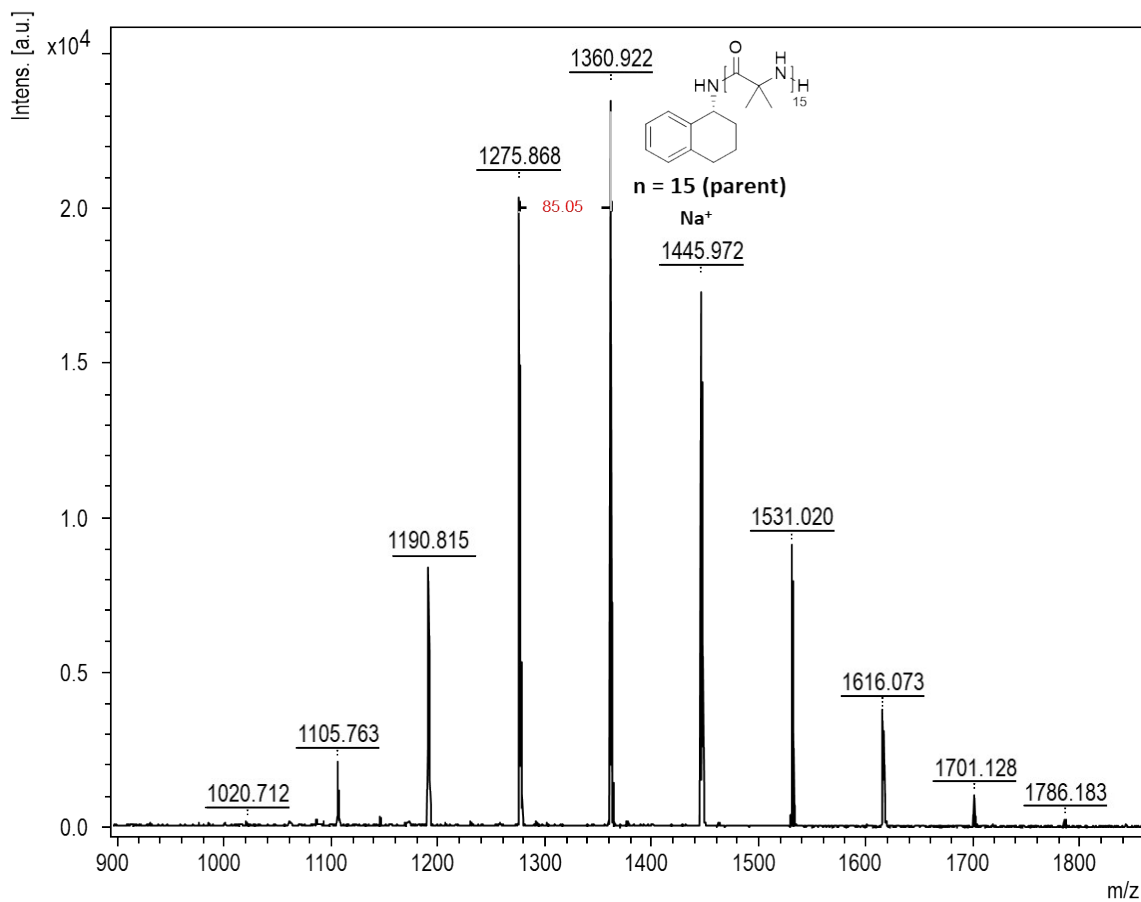
End-group conversion (%) was quantified from MALDI-TOF MS by comparing the signal intensity of the modified chains to the sum of the modified and unmodified chains for the same degree of polymerisation (DP) and the same alkali adduct. The percentage conversion was calculated according to the following formula:

$$\text{Conv. \%} = \frac{I_{\text{mod}}(n, M + \text{Cat}^+)}{I_{\text{mod}}(n, M + \text{Cat}^+) + I_{\text{unmod}}(n, M + \text{Cat}^+)} \quad (1)$$

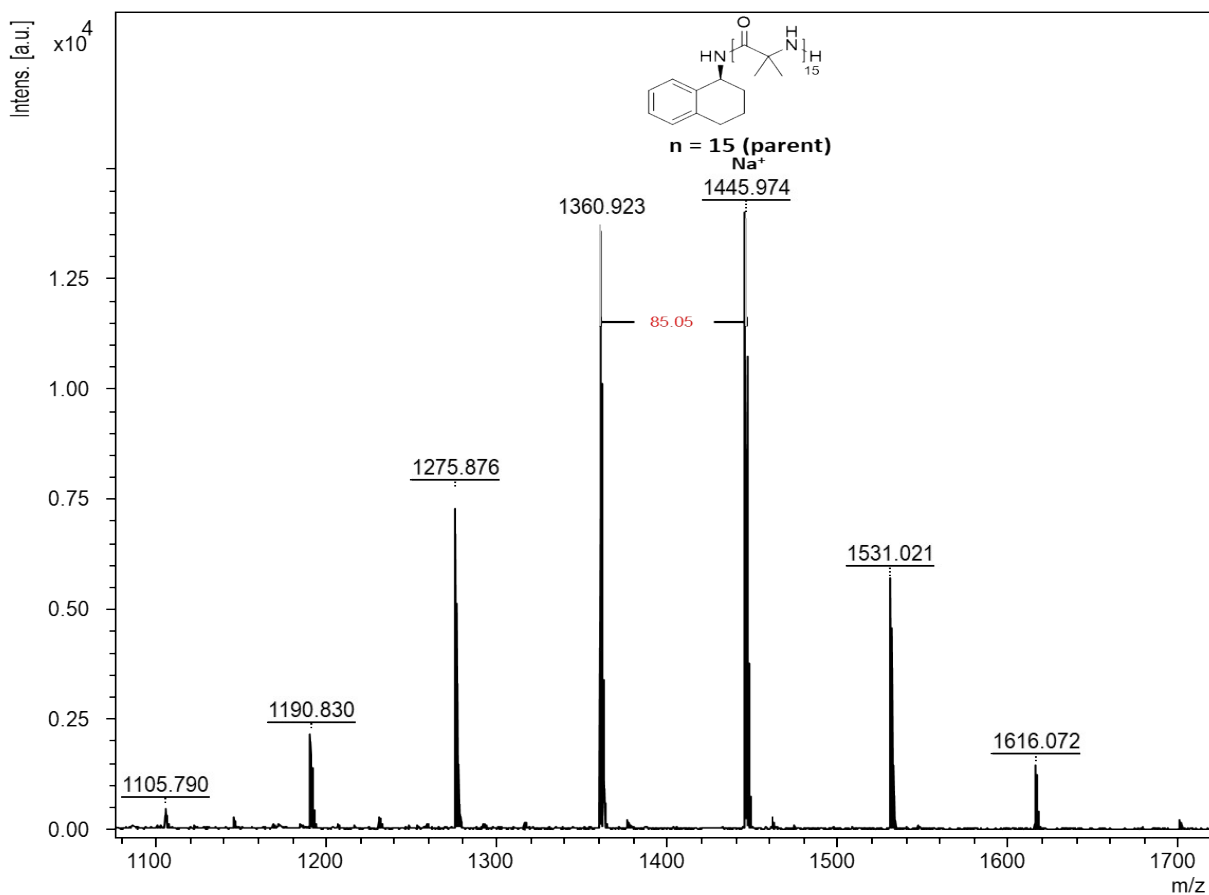
$I_{\text{mod}}(n, M + \text{Cat}^+)$ : Intensity of the modified chain at DP  $n$  (e.g., 15) detected as the same alkali adduct ( $\text{Na}^+$ ,  $\text{K}^+$ ,  $\text{Li}^+$ ). DP ( $n$ ) was chosen where the isotope patterns of the modified and unmodified pairs were clearly resolved.

$I_{unmod}(n, M + Cat^+)$ : Intensity of the unmodified chain at the same DP and adduct ( $Na^+$ ,  $K^+$ ,  $Li^+$ ).

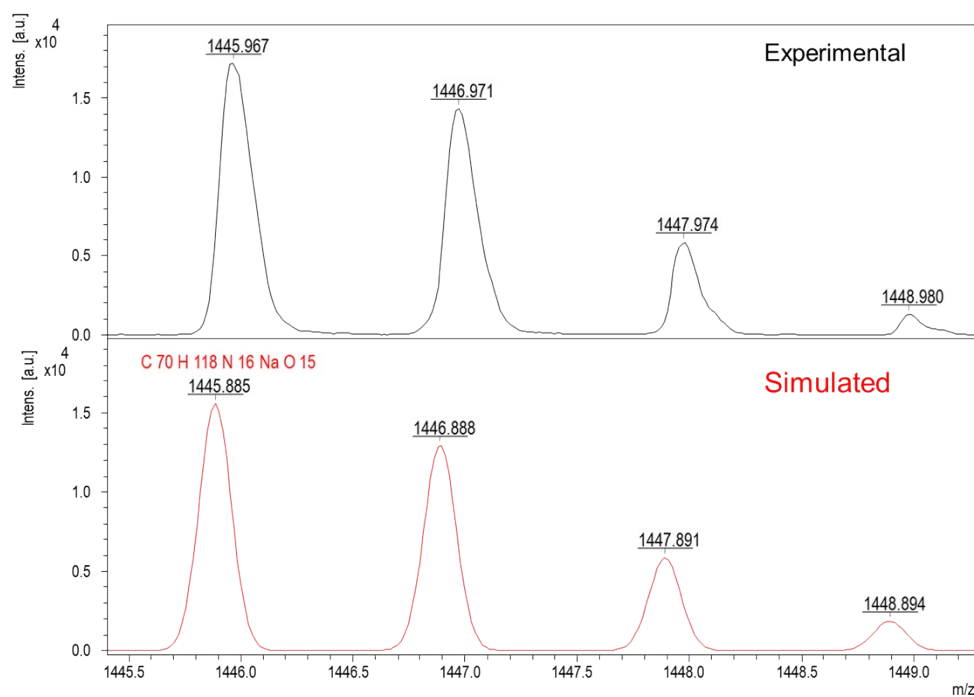
## MALDI-TOF MS Spectra and Simulations of Parent Polymers



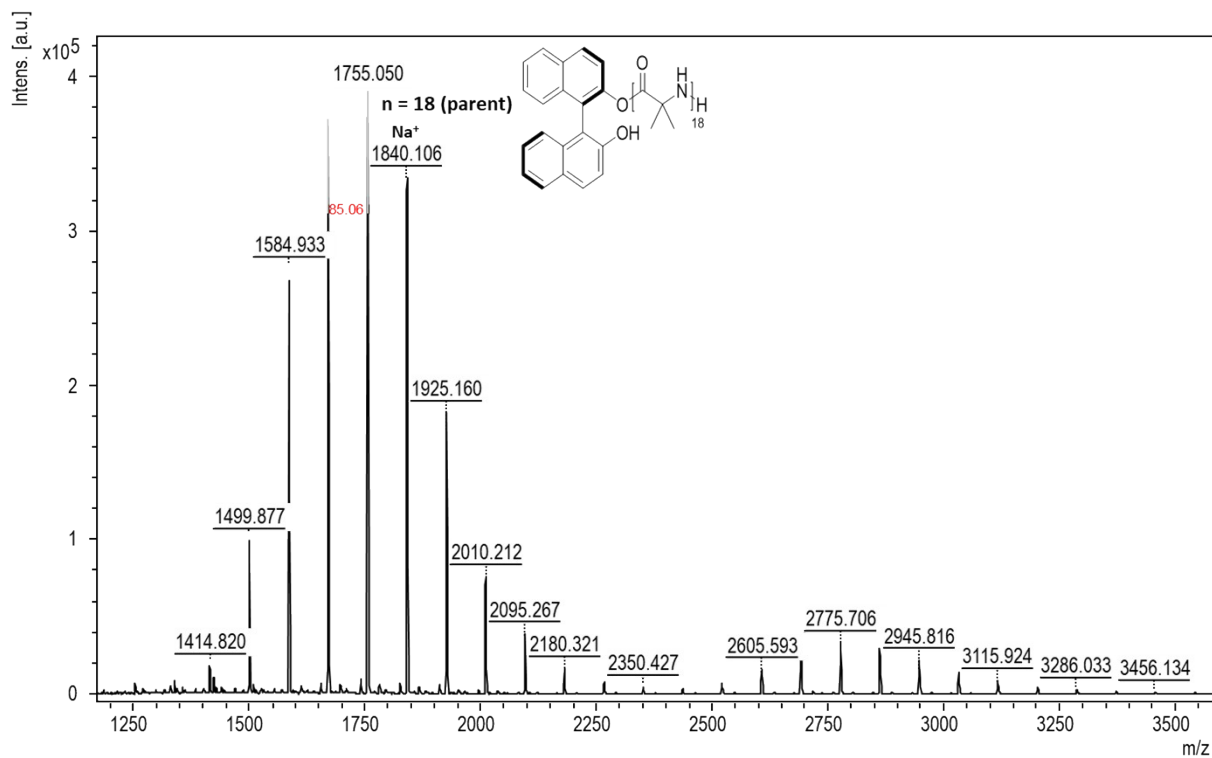
SI 24: MALDI TOF Spectra of parent polymer  $A^R-P_0-E_0$



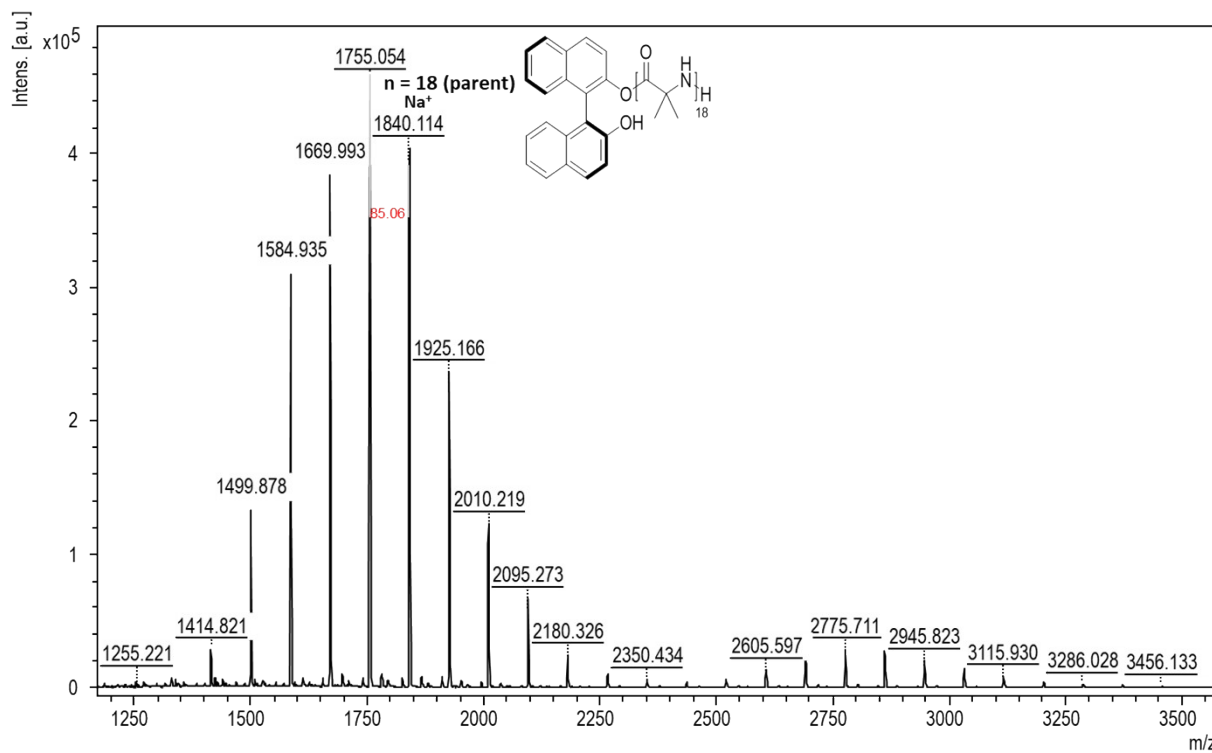
SI 25: MALDI TOF Spectra of parent polymer  $A^S\text{-}P_0\text{-}E_0$



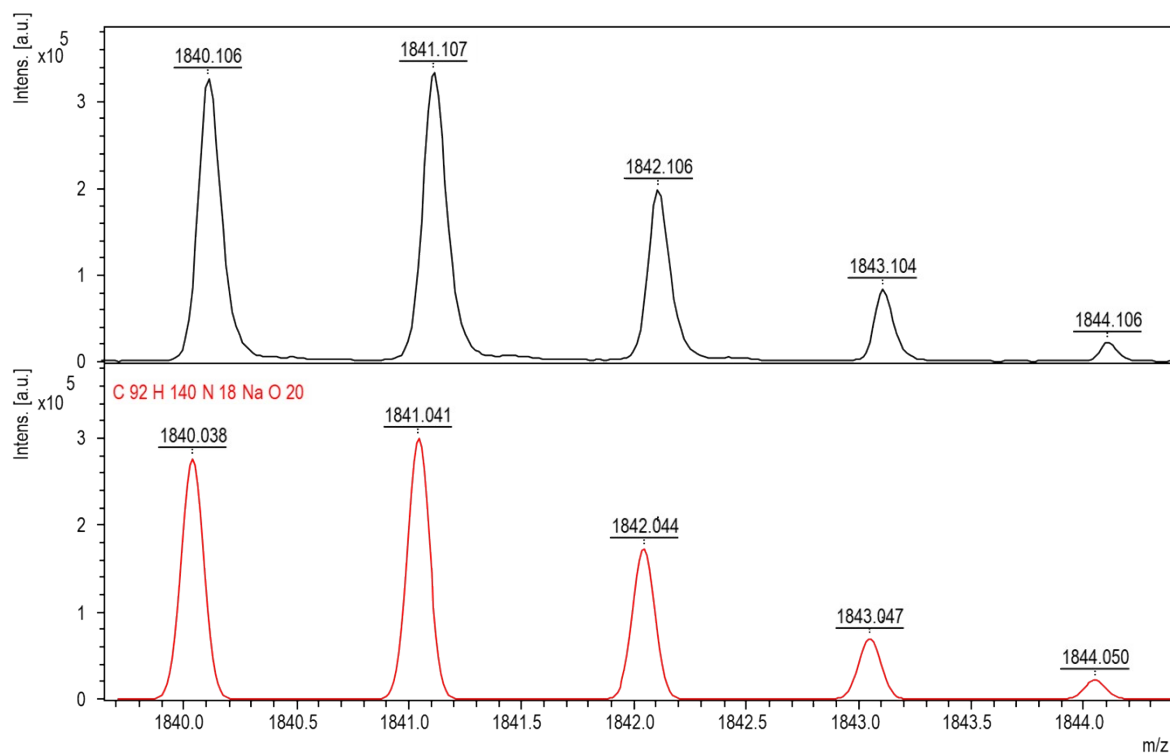
SI 26: 5 Experimental (Black) & Simulated (Red) Isotope pattern for unmodified parent polymer  $A^R\text{-}P_0\text{-}E_0$  with 15 repeating units +  $\text{Na}^+$



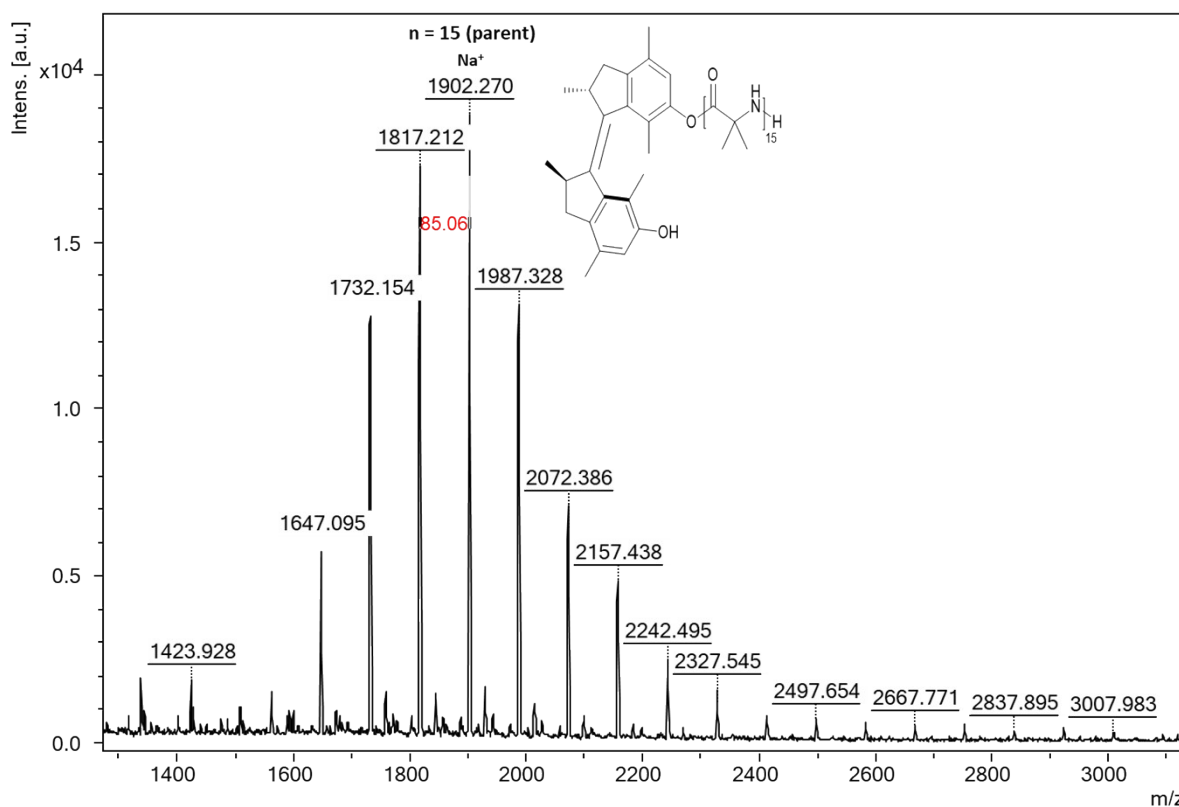
SI 27: MALDI TOF Spectra of parent polymer  $B^R-P_0-E_0$



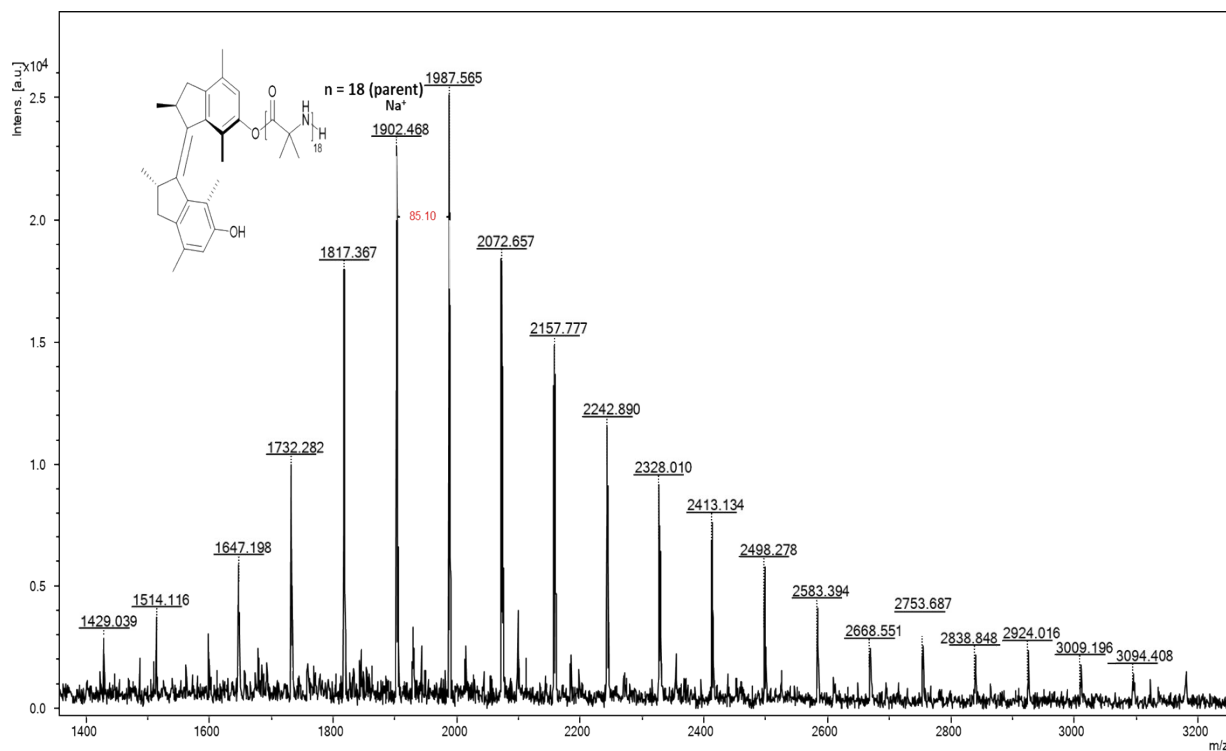
SI 28: MALDI TOF Spectra of parent polymer  $B^S-P_0-E_0$



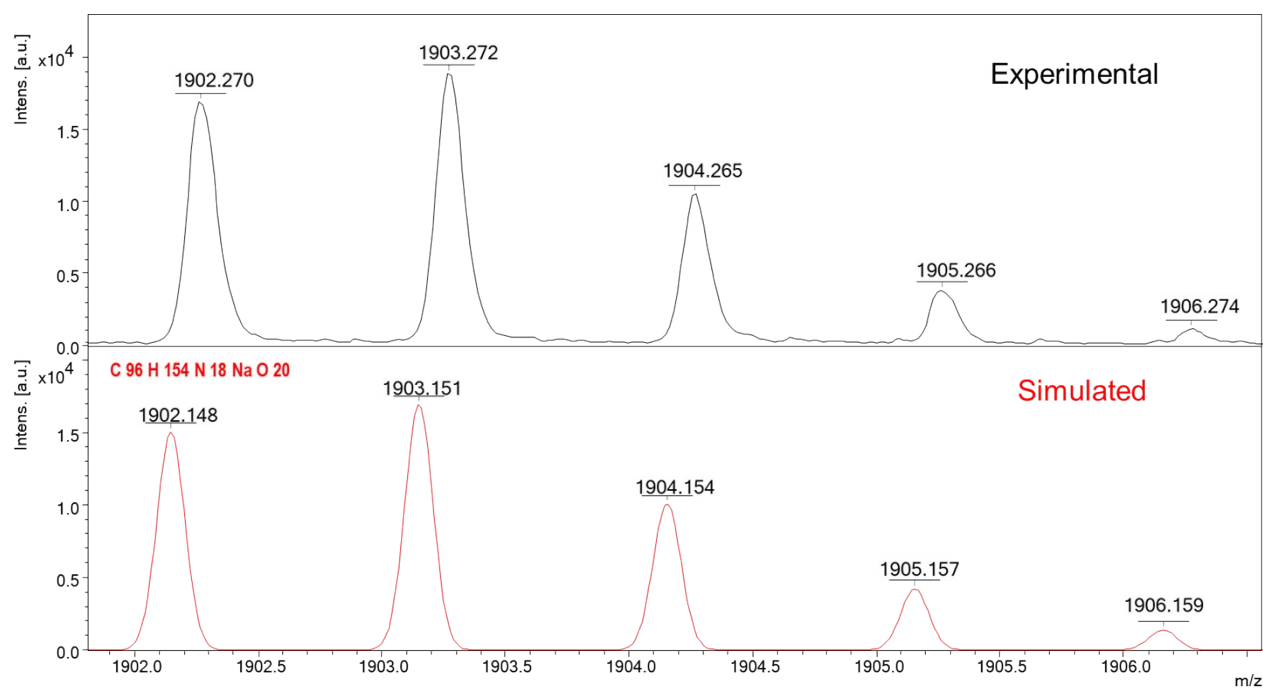
SI 29: Experimental (Black) & Simulated (Red) Isotope pattern for unmodified parent polymer  $B^R-P_0-E_0$  with 15 repeating units +  $Na^+$



SI 30: MALDI TOF Spectra of parent polymer  $C^R-P_0-E_0$

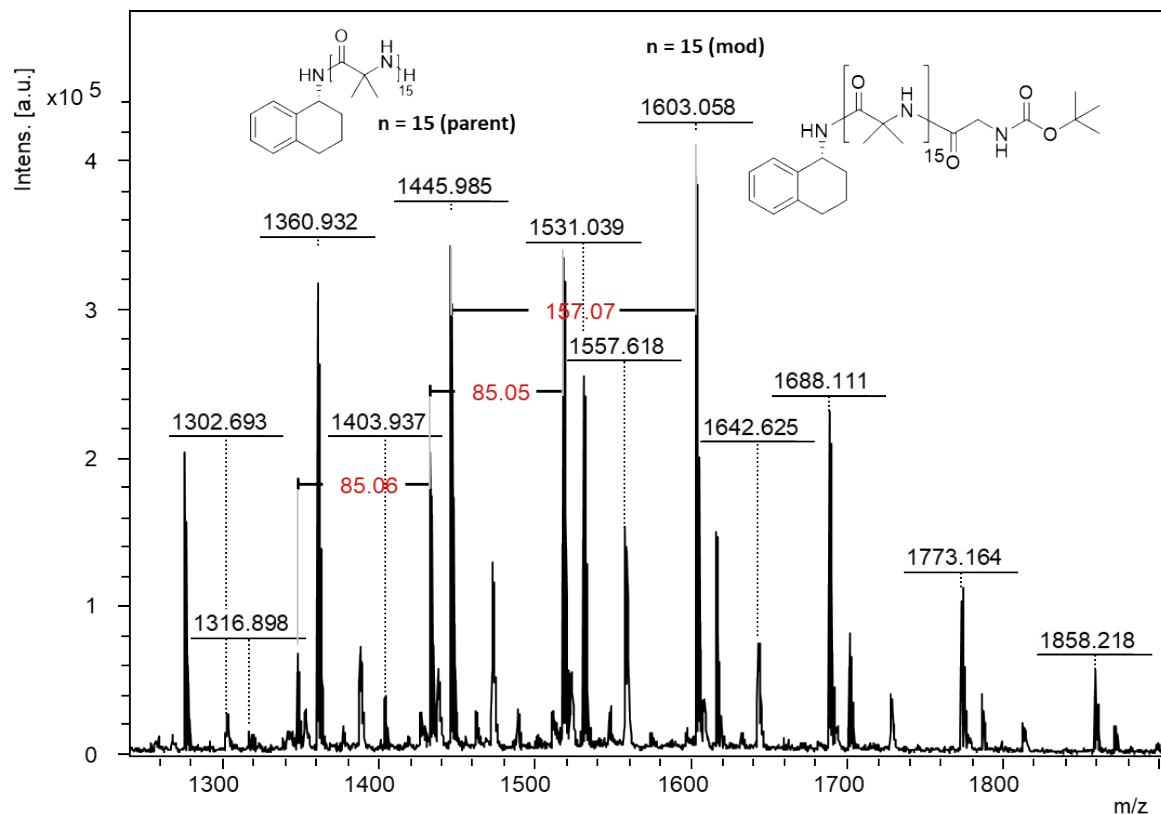


SI 31: MALDI TOF Spectra of parent polymer  $C^S-P_0-E_0$



SI 32: Experimental (Black) & Simulated (Red) Isotope pattern for unmodified parent polymer  $B^R-P_0-E_0$  with 15 repeating units +  $Na^+$

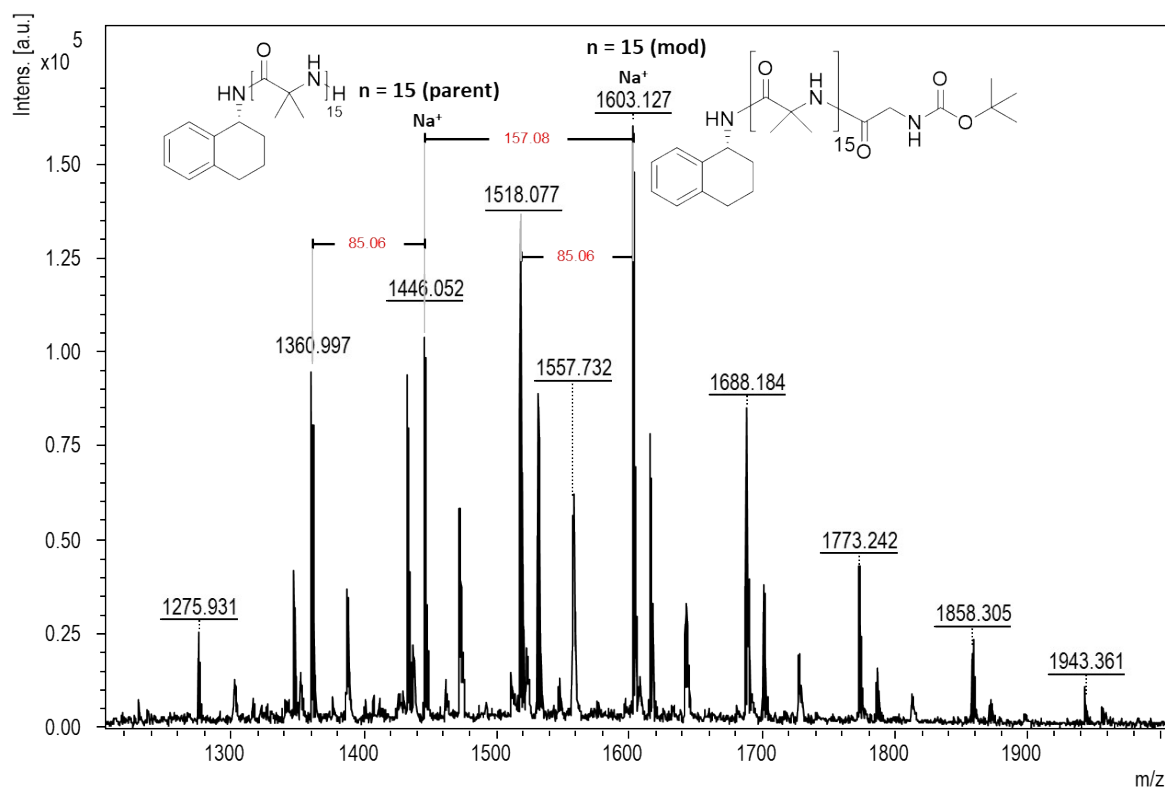
## MALDI-TOF MS Spectra and Simulations of Modified Polymers



SI 33: MALDI TOF Spectra of  $A^R-P_1-E_3$

Polymer	DP	Adduct	Parent Peak (m/z), Intensity $I_{umod}(n, M + Ca)$	Modified Peak (m/z), Intensity $I_{mod}(n, M + Cat)$	Approximate Conversion (%)
$A^R-P_1-E_3$	15	$Na^+$	1445.985, 362655	1603.059, 405715	53

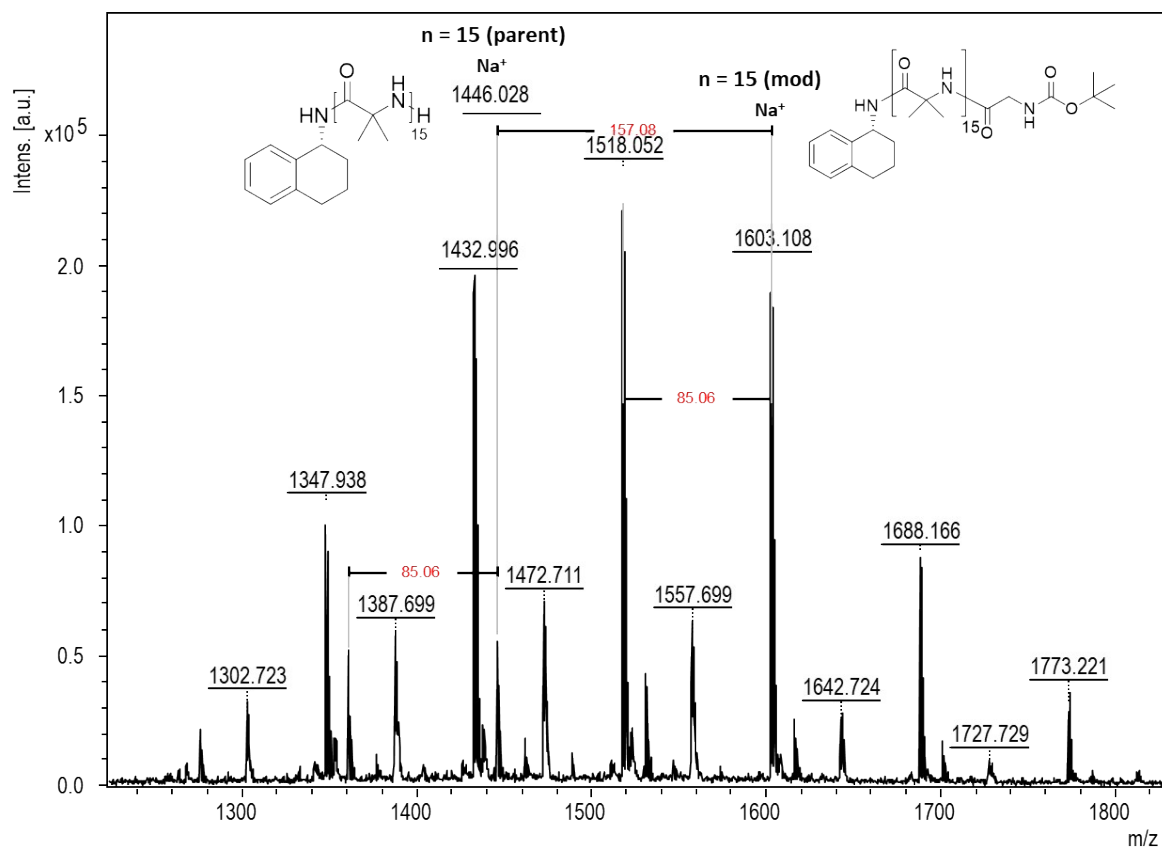
Using formula (1), the percentage conversion was calculated as 53%.



SI 34: MALDI-TOF Spectra of  $A^R-P_2-E_3$

Polymer	DP	Adduct	Parent Peak (m/z), Intensity $I_{umod}(n, M + Ca)$	Modified Peak (m/z), Intensity $I_{mod}(n, M + Cat)$	Approximate Conversion (%)
$A^R-P_2-E_3$	15	$Na^+$	1446.052, 109995	1603.127, 160013	60

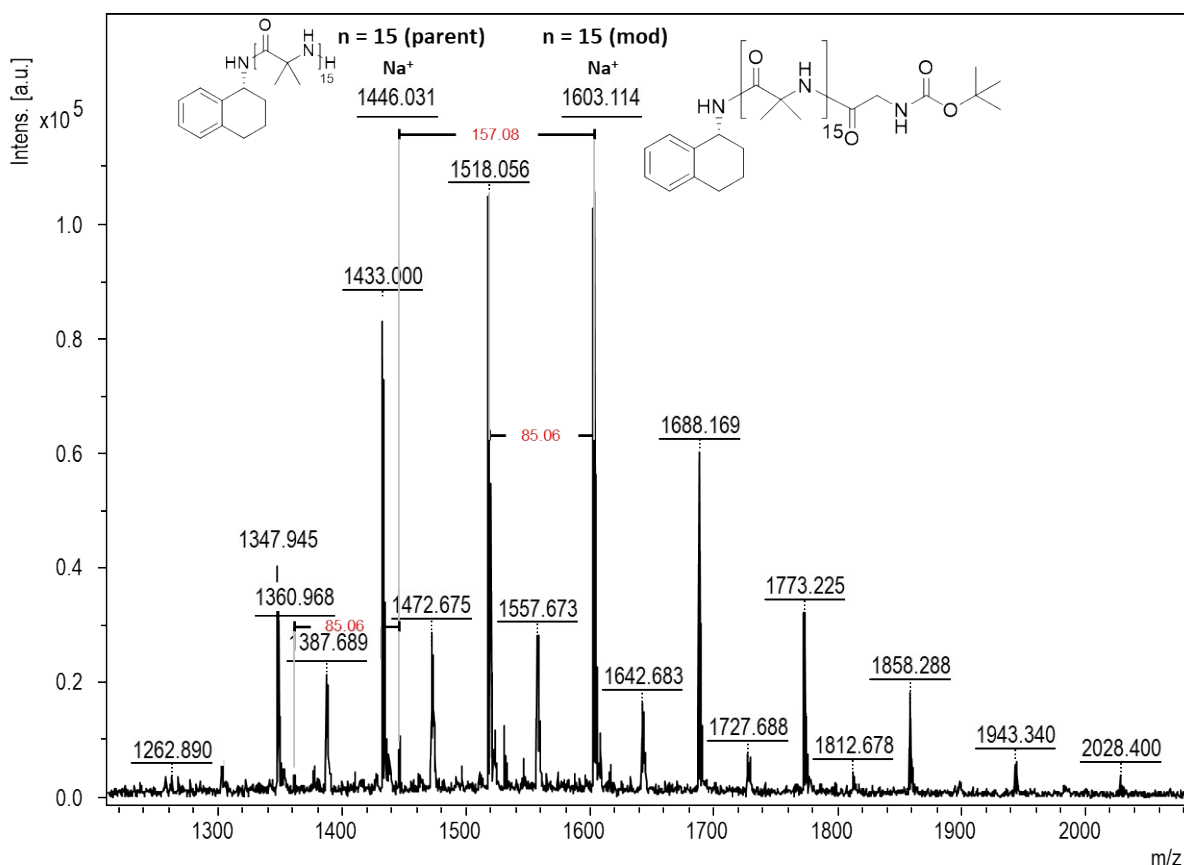
Using formula (1), the percentage conversion was calculated as 60%.



SI 35 MALDI-TOF Spectra of  $A^R-P_3-E_3$

Polymer	DP	Adduct	Parent Peak (m/z), Intensity $I_{unmod}(n, M + Ca)$	Modified Peak (m/z), Intensity $I_{mod}(n, M + Ca)$	Approximate Conversion (%)
$A^R-P_3-E_3$	15	$Na^+$	1446.028, 52289	1603.108, 200396	79

Using formula (1), the percentage conversion was calculated as 79%.

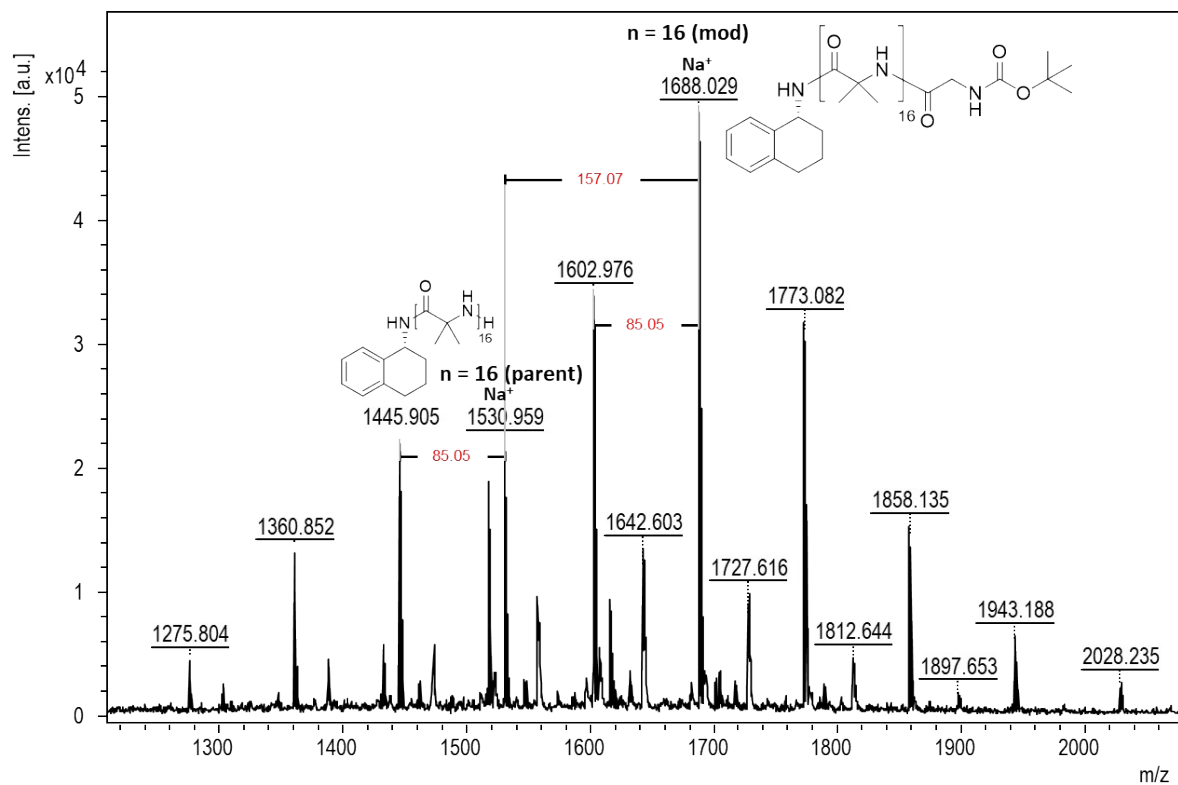


SI 36: MALDI-TOF Spectra of  $A^R-P_4-E_3$

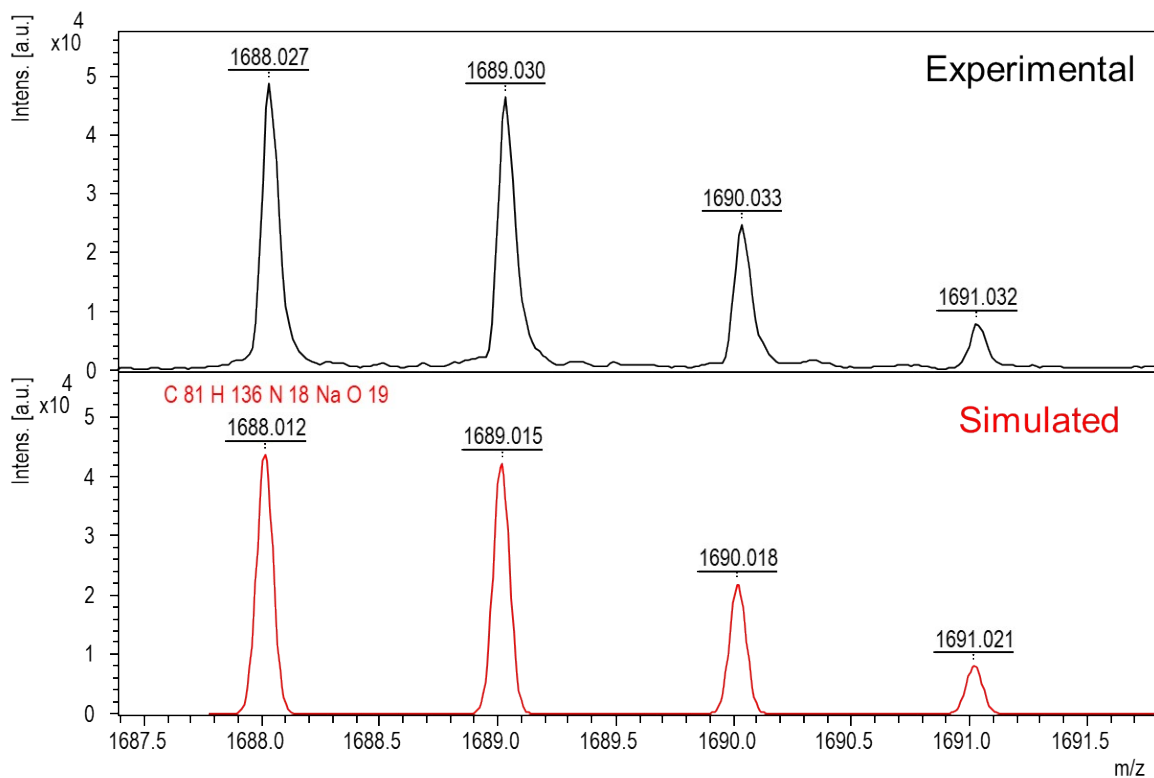
Polymer	DP	Adduct	Parent Peak (m/z), Intensity $I_{umod}(n, M + Ca)$	Modified Peak (m/z), Intensity $I_{mod}(n, M + Ca)$	Approximate Conversion (%)
$A^R-P_4-E_3$	15	$Na^+$	1446.031, 9388	1603.114, 108191	92

Using formula (1), the percentage conversion was calculated as 92%.

**Boc-Deprotection of  $A^R-P_4-E_3$ :**  $A^R-P_4-E_3$  (50.1 mg, 0.0368 mmol) was dissolved in HFIP (1800  $\mu$ L), and distilled water (200  $\mu$ L) was added under stirring. After cooling to 0°C, TFA (3  $\mu$ L, 1.06 eq) was added, and the solution was allowed to warm to room temperature and stirred for 3 days under  $N_2$ . The solvents were concentrated under vacuum, leaving a white solid, which was further dried using a high-vacuum pump. The MALDI-TOF MS spectrum of the resulting deprotected polymer is shown in SI 38.



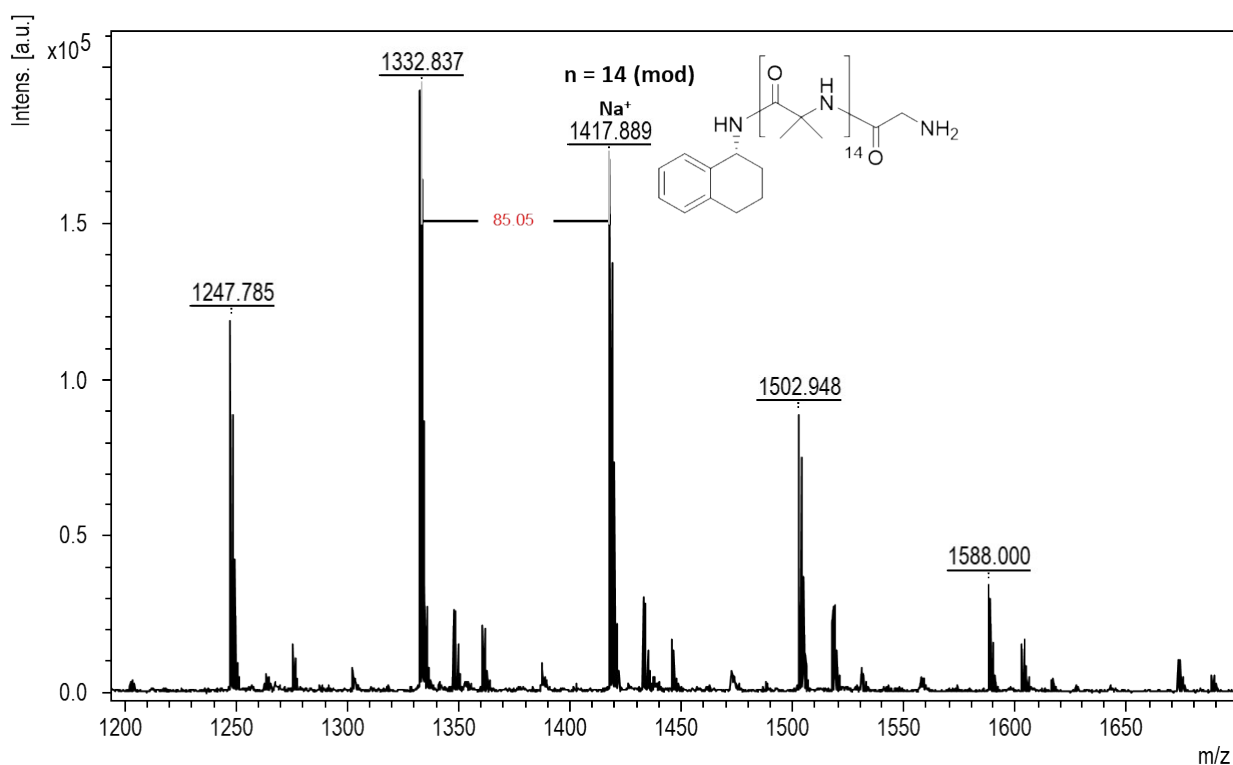
SI 37: MALDI Spectra of A<sup>S</sup>-P<sub>5</sub>-E<sub>3</sub>



SI 38 Experimental (Black) & Simulated (Red) Isotope pattern for modified polymer A<sup>S</sup>-P<sub>5</sub>-E<sub>3</sub> with 16 repeating units + Na<sup>+</sup>

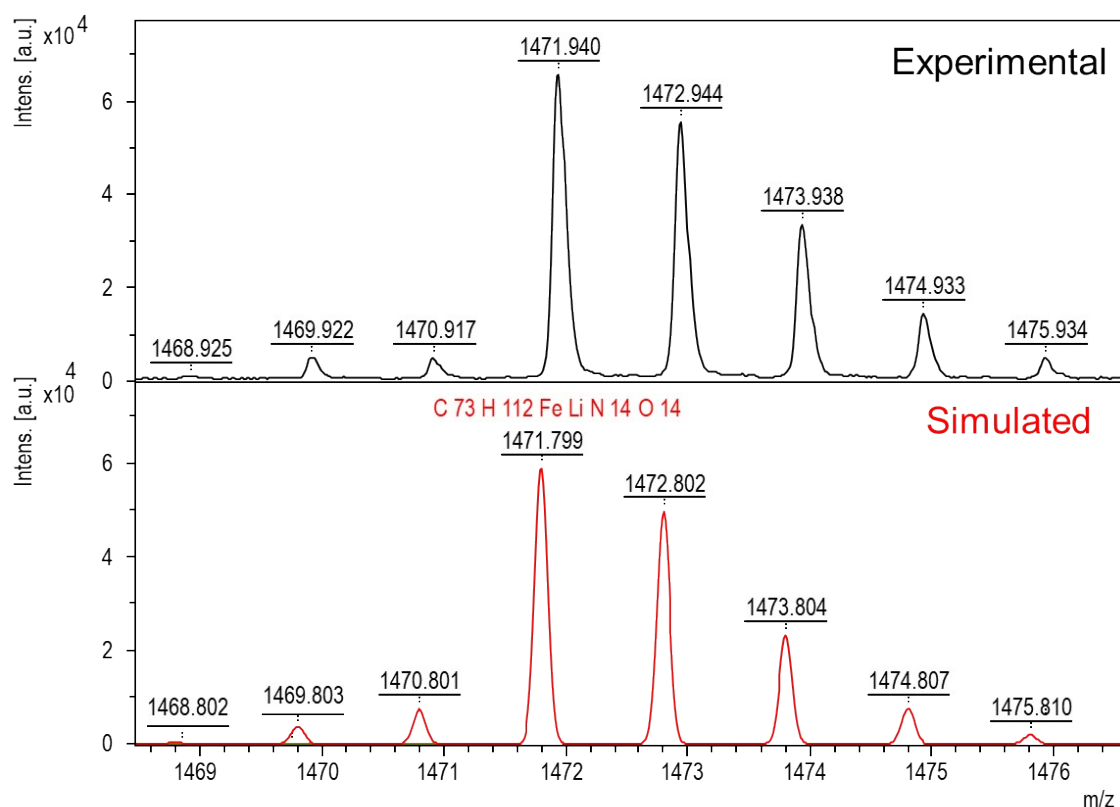
Polymer	DP	Adduct	Parent Peak (m/z), Intensity $I_{umod}(n, M + Ca)$	Modified Peak (m/z), Intensity $I_{mod}(n, M + Cat)$	Approximate Conversion (%)
<b>A<sup>S</sup>-P<sub>5</sub>-E<sub>3</sub></b>	16	Na <sup>+</sup>	1530.959, 21368	1688.029, 48611	69

Using formula (1), the percentage conversion was calculated as 69%.



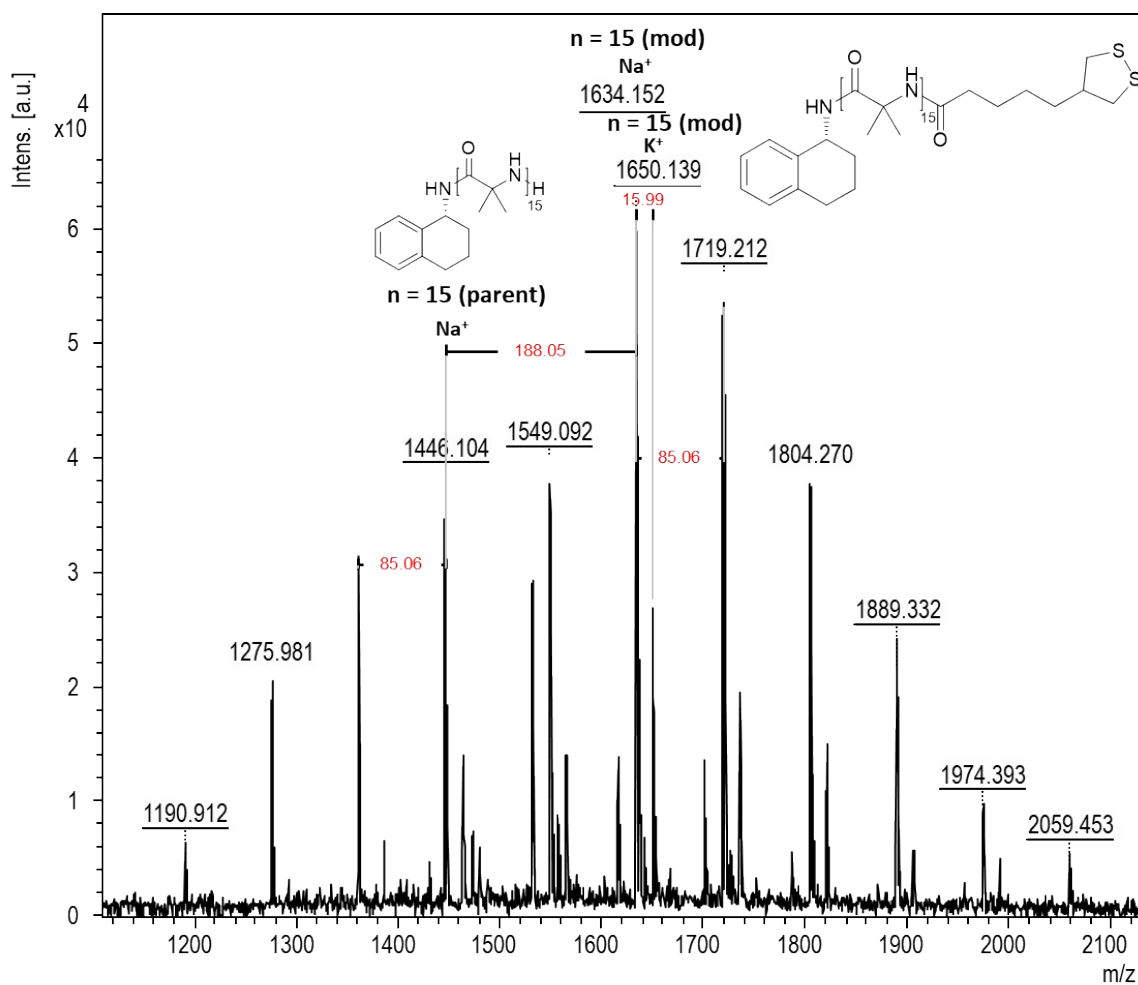
SI 39: MALDI-TOF Spectra of AR-P4-E3 after Boc deprotection (TFA, HFIP/H<sub>2</sub>O, 9:1 v/v)





SI 42: Experimental (Black) & Simulated (Red) Isotope pattern for modified polymer  $A^R\text{-P}_6\text{-E}_4$  with 13 repeating units +  $\text{Li}^+$

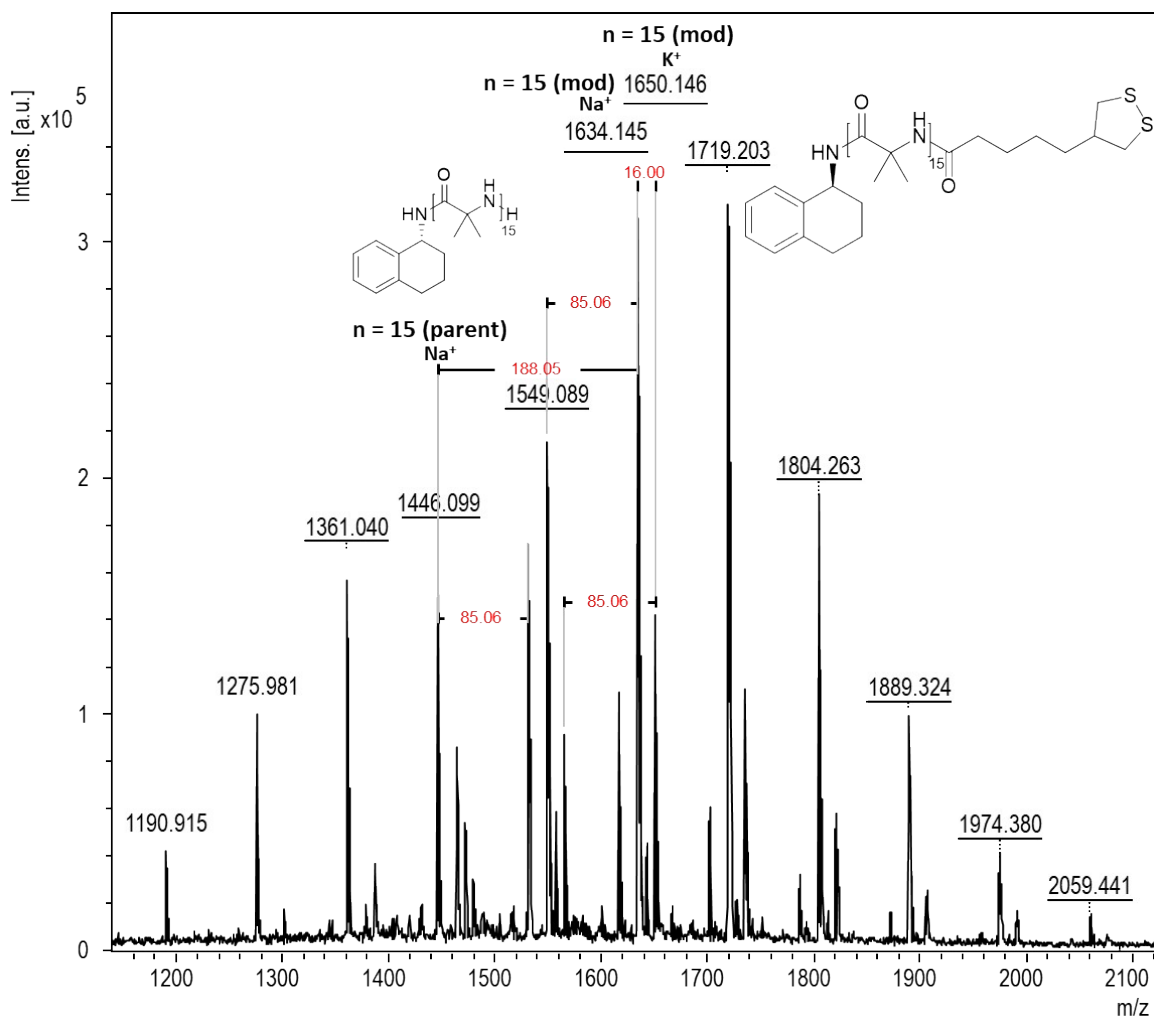
For polymers  $A^R\text{-P}_6\text{-E}_4$  and  $A^S\text{-P}_7\text{-E}_4$ , the MALDI-TOF MS spectra showed the main distribution of the modified polymers exclusively as  $\text{Li}^+$  adducts, while the corresponding  $\text{Li}^+$  series of the unmodified parent polymer was absent. This selective ionisation precluded reliable determination of conversion by MALDI; therefore,  $^1\text{H}$  NMR spectroscopy was employed to quantify end-group incorporation (see SI 18).



SI 43: MALDI-TOF Spectra of  $A^R-P_8-E_1$

Polymer	DP	Adduct	Parent Peak (m/z), Intensity $I_{umod}(n, M + Ca)$	Modified Peak (m/z), Intensity $I_{mod}(n, M + Cat)$	Approximate Conversion (%)
$A^R-P_8-E_1$	15	$Na^+$	1466.104, 38265	1688.029, 61390	62

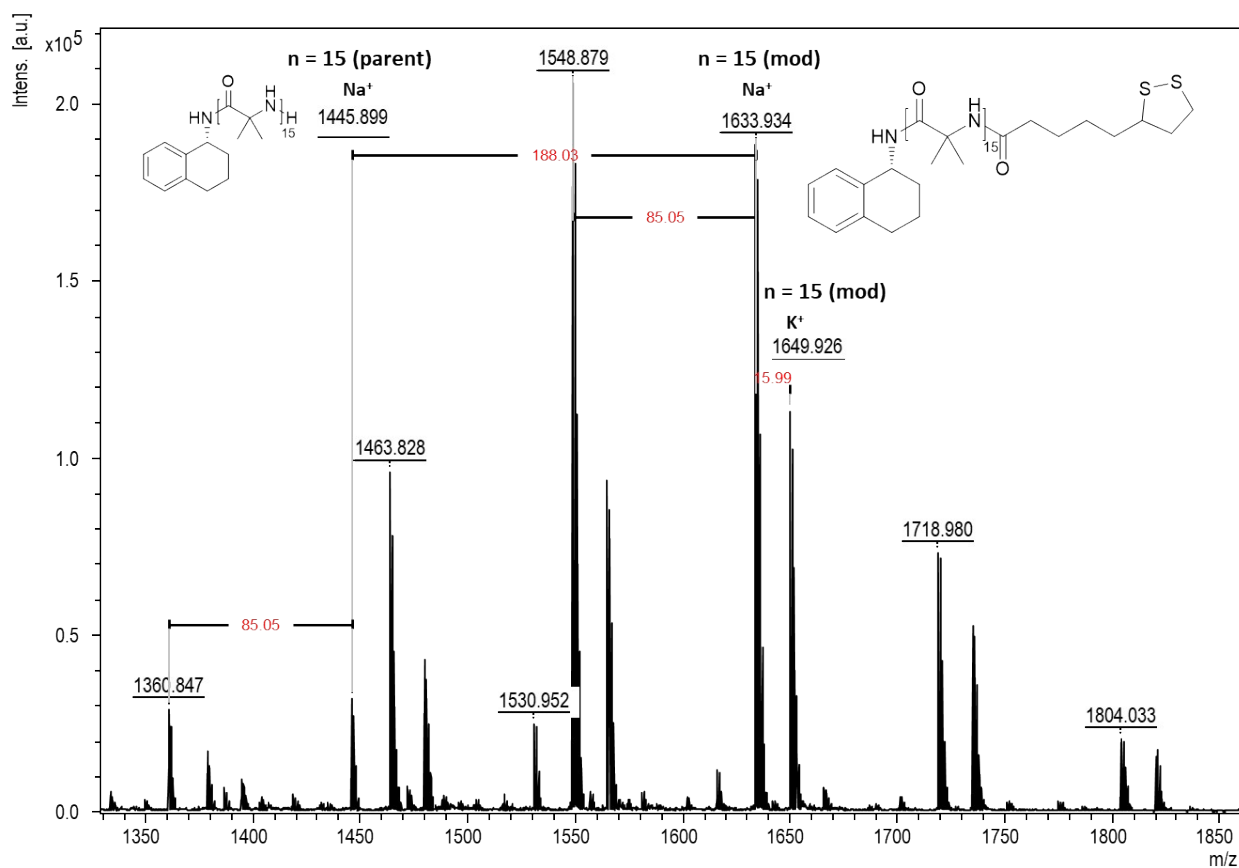
Using formula (1), the percentage conversion was calculated as 62%.



SI 44: MALDI-TOF Spectra of  $A^R-P_9-E_1$

Polymer	DP	Adduct	Parent Peak (m/z), Intensity $I_{umod}(n, M + Ca)$	Modified Peak (m/z), Intensity $I_{mod}(n, M + Cat)$	Approximate Conversion (%)
$A^R-P_9-E_1$	15	$Na^+$	1466.099, 177329	1634.145, 318880	64

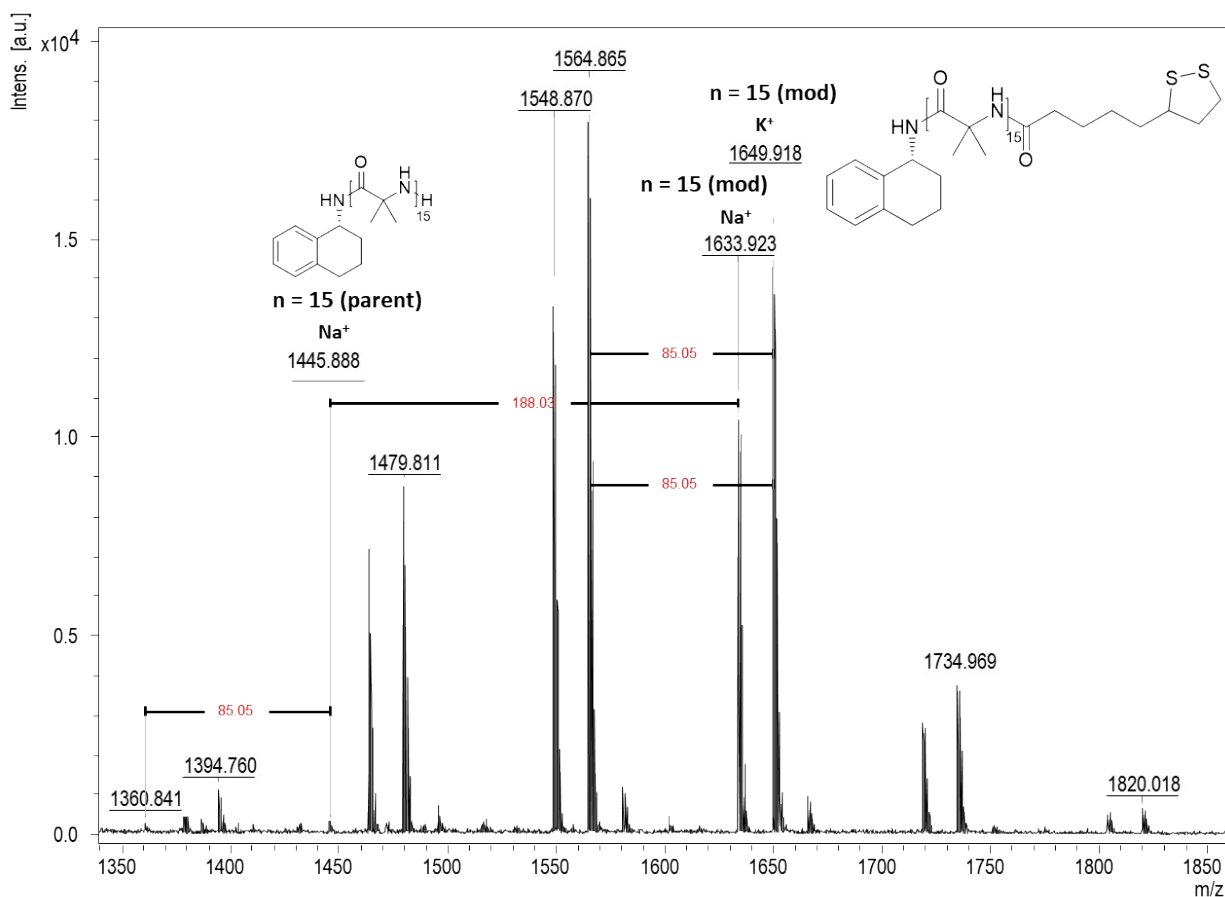
Using formula (1), the percentage conversion was calculated as 64%.



SI 45: MALDI-TOF Spectra of  $A^R-P_{10}-E_2$

Polymer	DP	Adduct	Parent Peak (m/z), Intensity $I_{umod}(n, M + Ca)$	Modified Peak (m/z), Intensity $I_{mod}(n, M + Cat)$	Approximate Conversion (%)
$A^R-P_{10}-E_2$	15	Na <sup>+</sup>	1445.899, 32123	1633.934, 188576	85

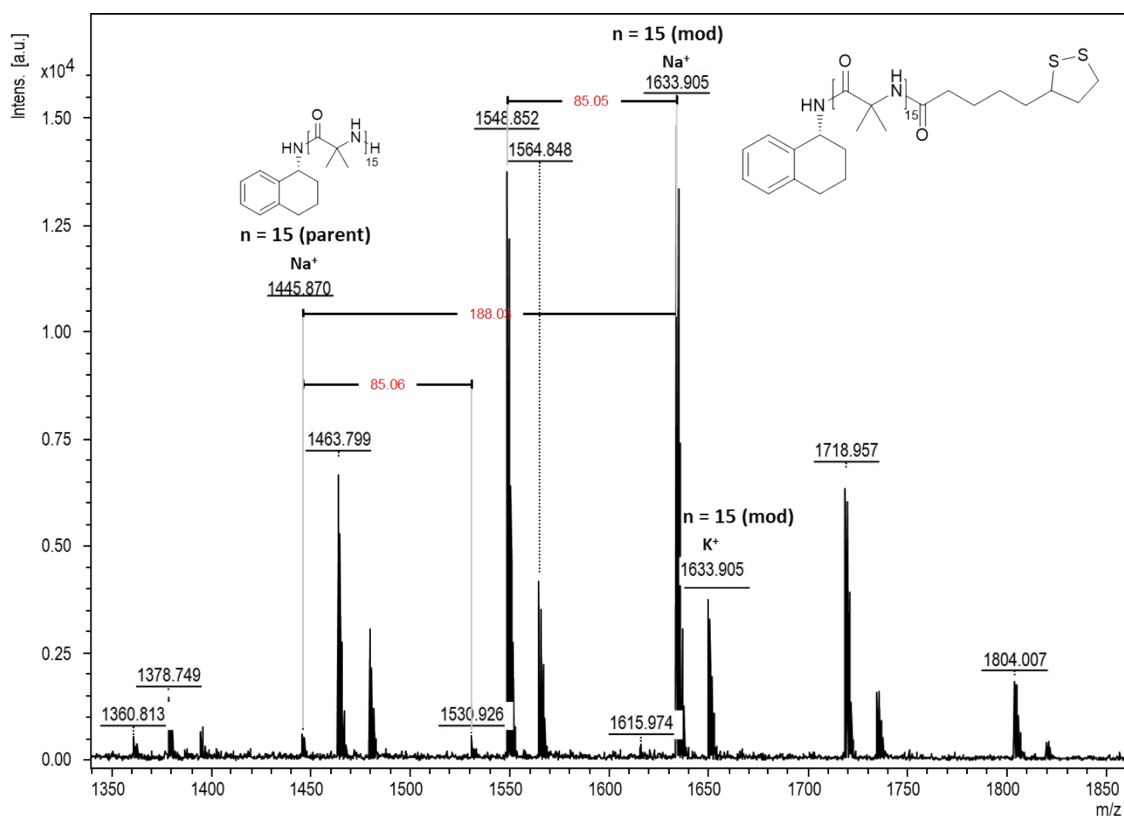
Using formula (1), the percentage conversion was calculated as 85%.



SI 46: MALDI TOF Spectra of  $A^R-P_{11}-E_2$

Polymer	DP	Adduct	Parent Peak (m/z), Intensity $I_{umod}(n, M + Ca)$	Modified Peak (m/z), Intensity $I_{mod}(n, M + Cat)$	Approximate Conversion (%)
$A^R-P_{11}-E_2$	15	$Na^+$	1445.888, 297	1633.923, 11044	97

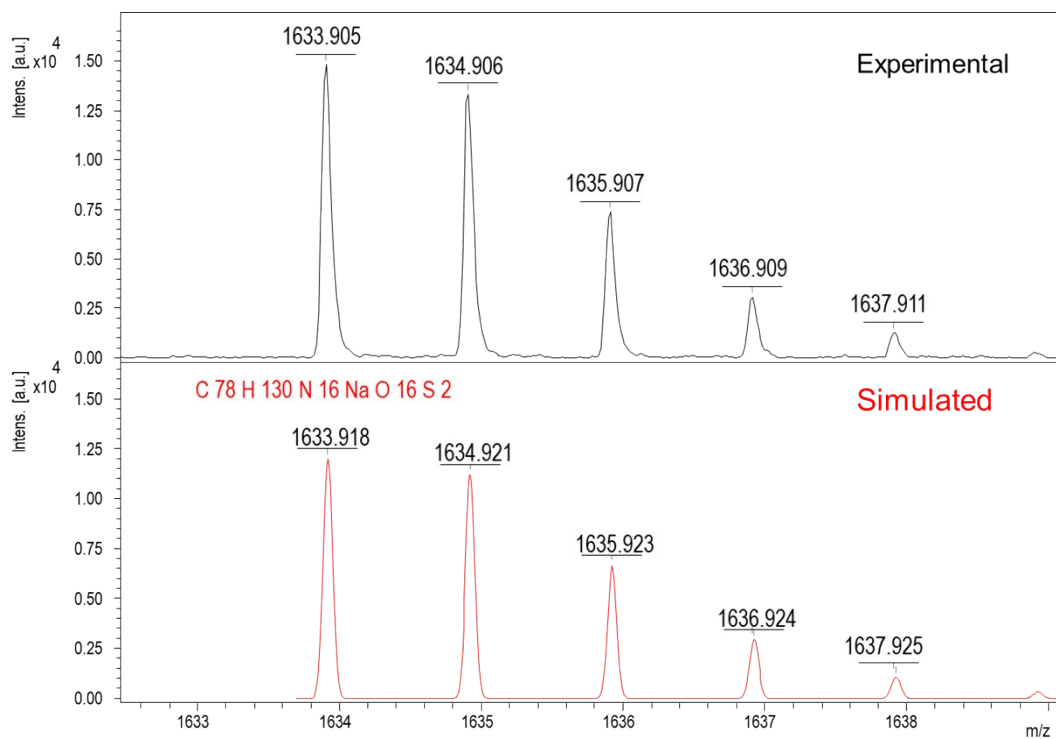
Using formula (1), the percentage conversion was calculated as 97%.



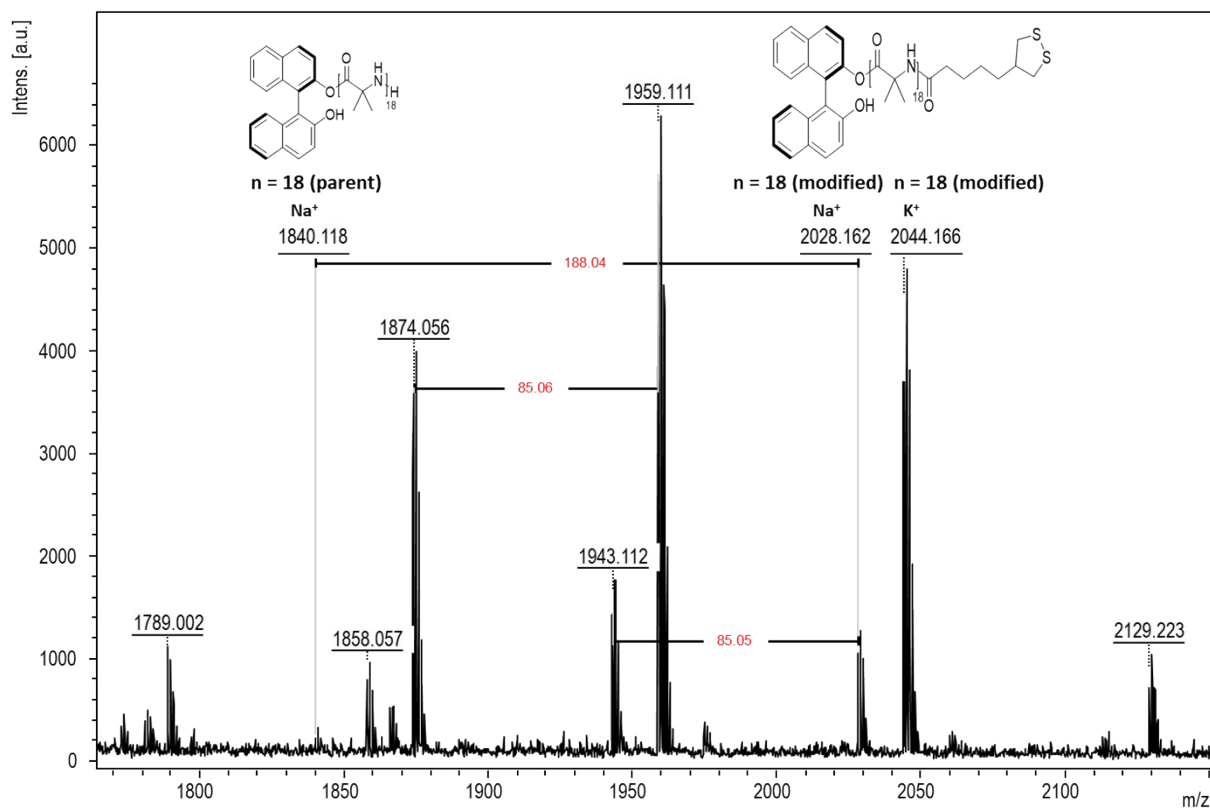
SI 47 MALDI-TOF Spectra of  $A^R-P_{12}-E_2$

Polymer	DP	Adduct	Parent Peak (m/z), Intensity $I_{umod}(n, M + Ca)$	Modified Peak (m/z), Intensity $I_{mod}(n, M + Cat)$	Approximate Conversion (%)
$A^R-P_{12}-E_2$	13	$Na^+$	1275.770, 379	1463.799, 6964	95
$A^R-P_{12}-E_2$	14	$Na^+$	1360.813, 471	1548.852, 14493	97
$A^R-P_{12}-E_2$	15	$Na^+$	1445.870, 588	1633.905, 15315	96
$A^R-P_{12}-E_2$	16	$Na^+$	1530.926, 430	1718.957, 6715	94
$A^R-P_{12}-E_2$	17	$Na^+$	1615.974, 236	1804.007, 2869	92

Using formula (1), the percentage conversion was calculated as 96%.



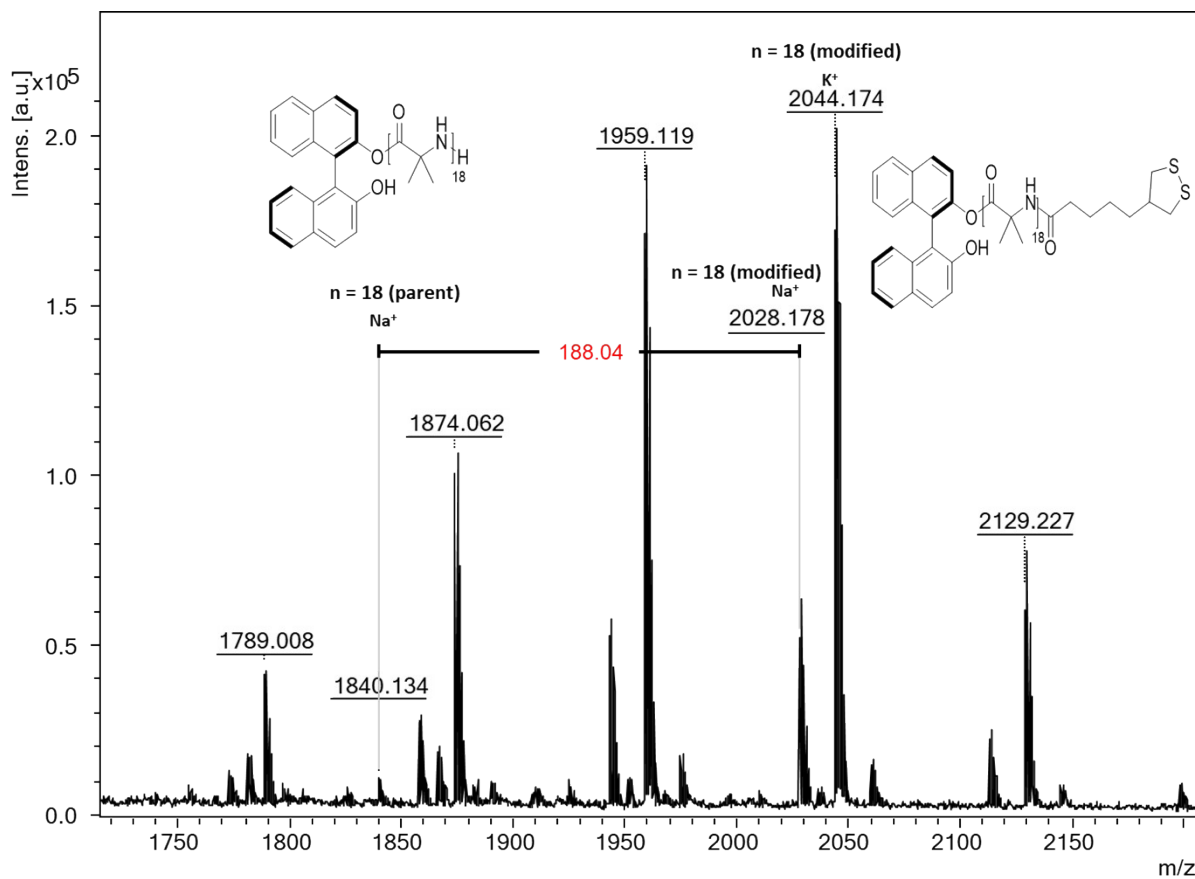
SI 48: Experimental (Black) & Simulated (Red) Isotope pattern for modified polymer  $A^R-P_{12}-E_2$  with 15 repeating units +  $Na^+$



SI 49: MALDI TOF Spectra of  $B^R-P_{13}-E_1$

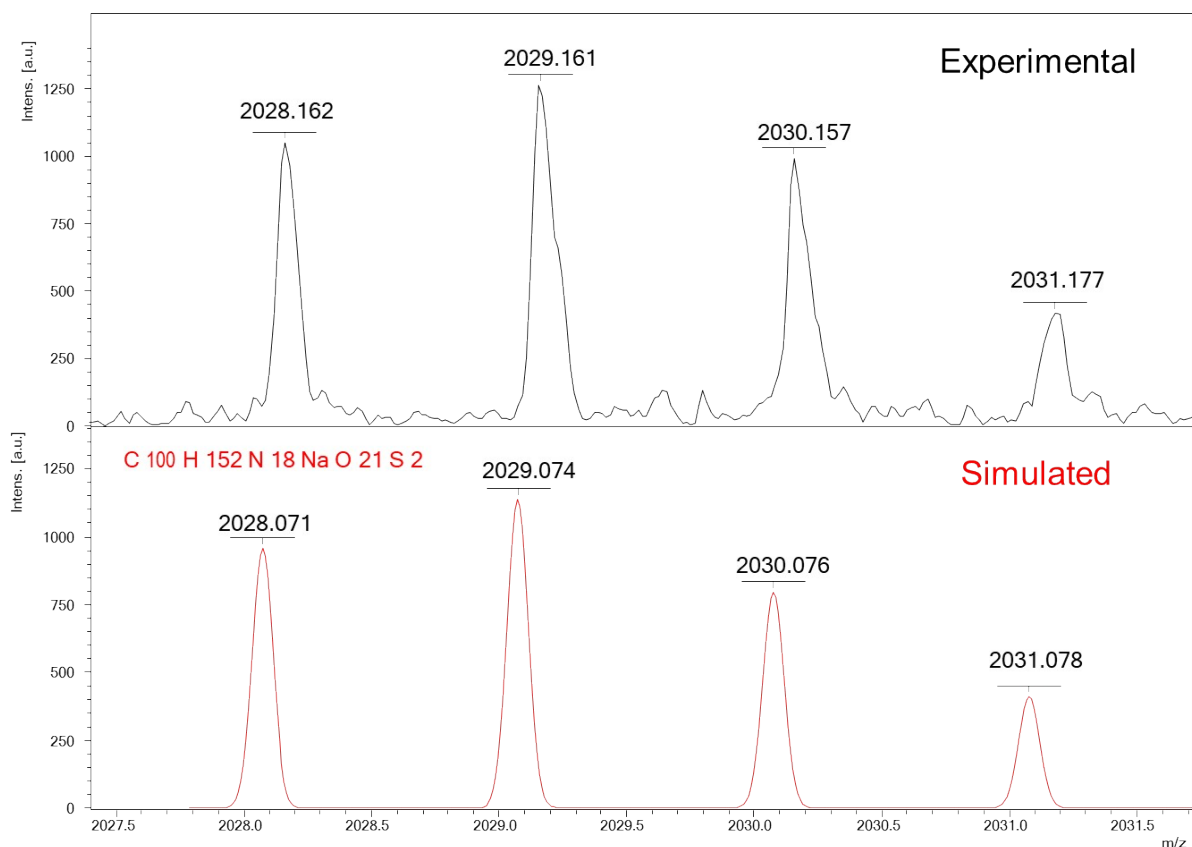
Polymer	DP	Adduct	Parent Peak (m/z), Intensity $I_{unmod}(n, M + Ca)$	Modified Peak (m/z), Intensity $I_{mod}(n, M + Cat)$	Approximate Conversion (%)
$B^R-P_{13}-E_1$	18	Na <sup>+</sup>	1840.118, 212	2028.162, 1048	83

Using formula (1), the percentage conversion was calculated as 83%.

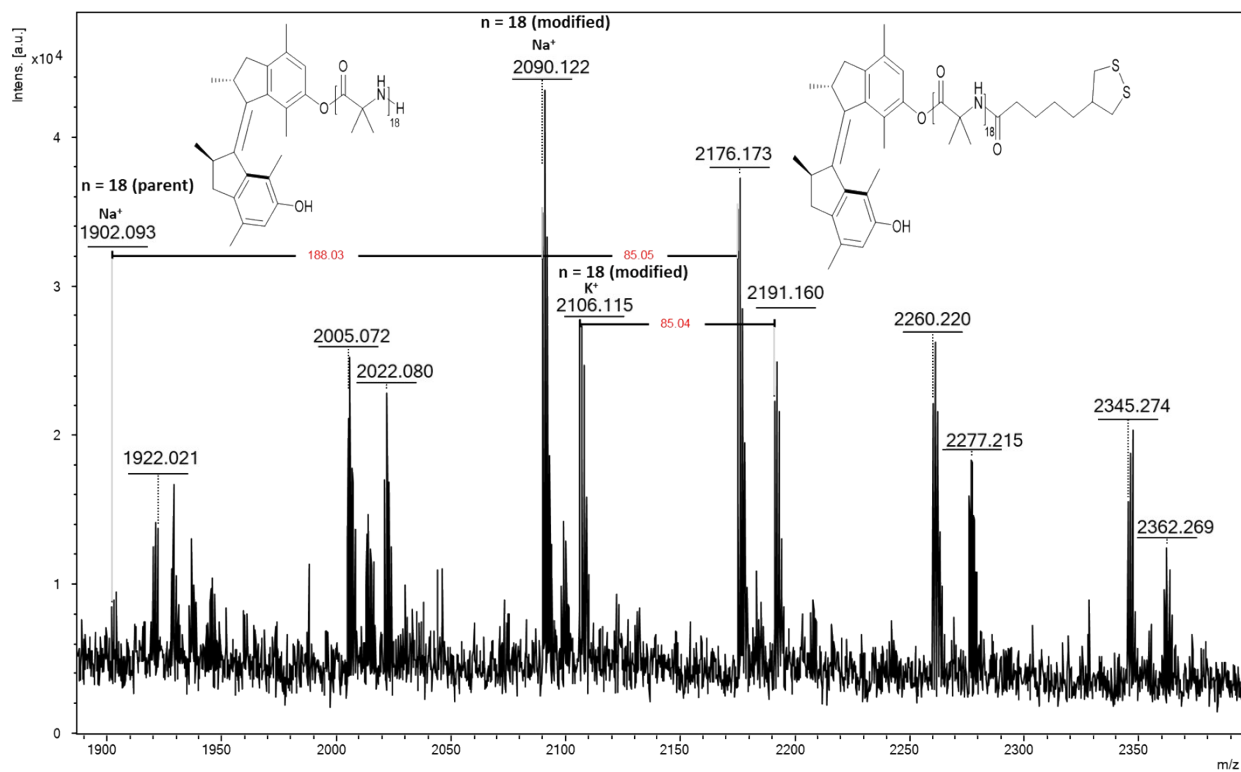


Polymer	DP	Adduct	Parent Peak (m/z), Intensity $I_{umod}(n, M + Ca)$	Modified Peak (m/z), Intensity $I_{mod}(n, M + Cat)$	Approximate Conversion (%)
$B^S-P_{14}-E_1$	18	$Na^+$	1840.134, 11122	2028.178, 57384	83

Using formula (1), the percentage conversion was calculated as 83%.



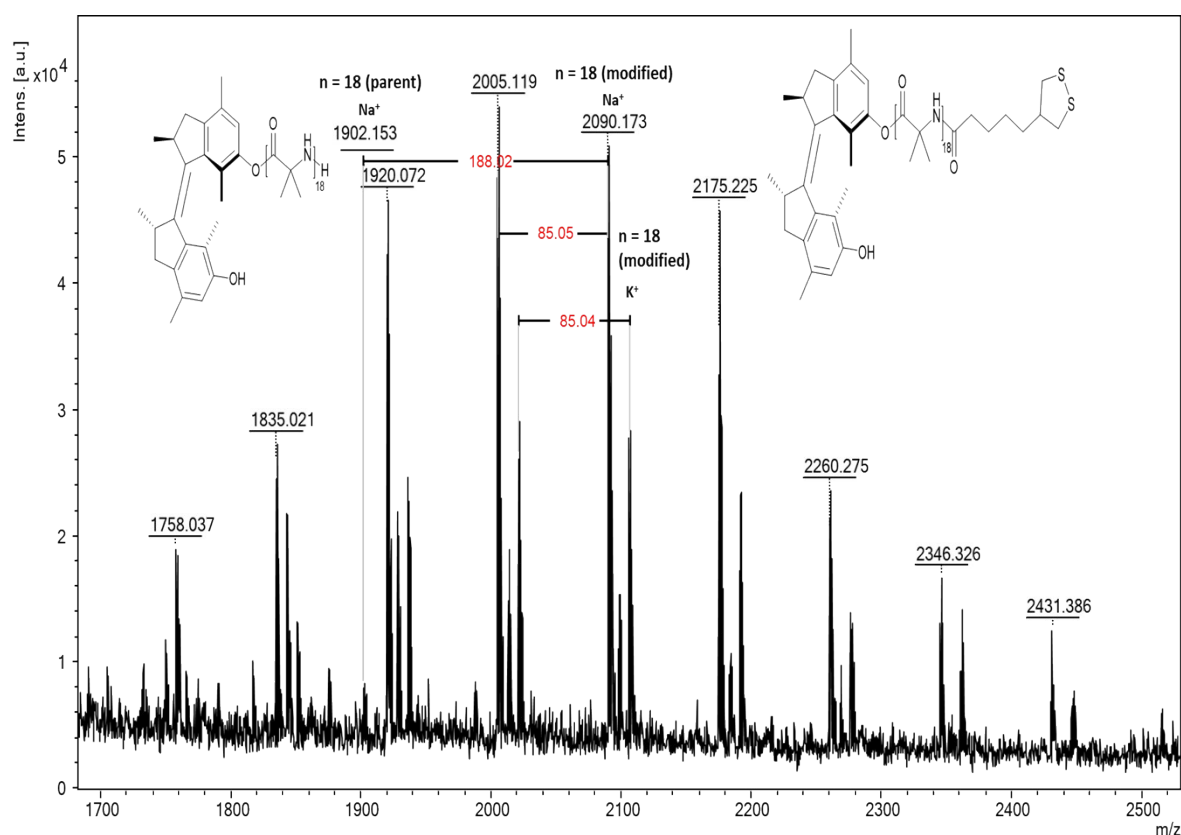
SI 51 Experimental (Black) & Simulated (Red) Isotope pattern for modified polymer  $B^R-P_{13}-E_1$  with 18 repeating units +  $Na^+$



SI 52 MALDI TOF Spectra of  $C^R-P_{15}-E_1$

Polymer	DP	Adduct	Parent Peak (m/z), Intensity $I_{umod}(n, M + Ca)$	Modified Peak (m/z), Intensity $I_{mod}(n, M + Cat)$	Approximate Conversion (%)
<b>C<sup>R</sup>-P<sub>15</sub>-E<sub>1</sub></b>	18	Na <sup>+</sup>	1902.093, 8431	2090.122, 37911	82

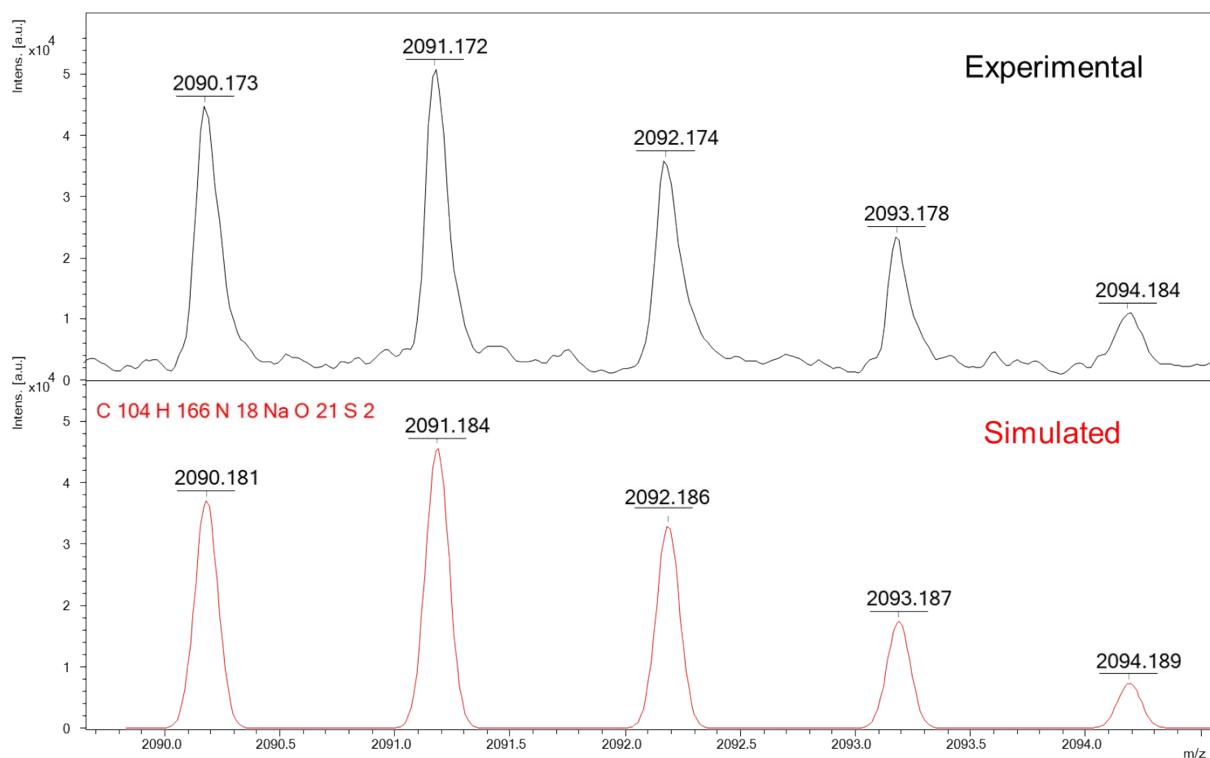
Using formula (1), the percentage conversion was calculated as 82%.



Polymer	DP	Adduct	Parent Peak (m/z), Intensity $I_{umod}(n, M + Ca)$	Modified Peak (m/z), Intensity $I_{mod}(n, M + Cat)$	Approximate Conversion (%)
<b>C<sup>S</sup>-P<sub>16</sub>-E<sub>1</sub></b>	18	Na <sup>+</sup>	1902.153, 7939	2090.173, 46193	85

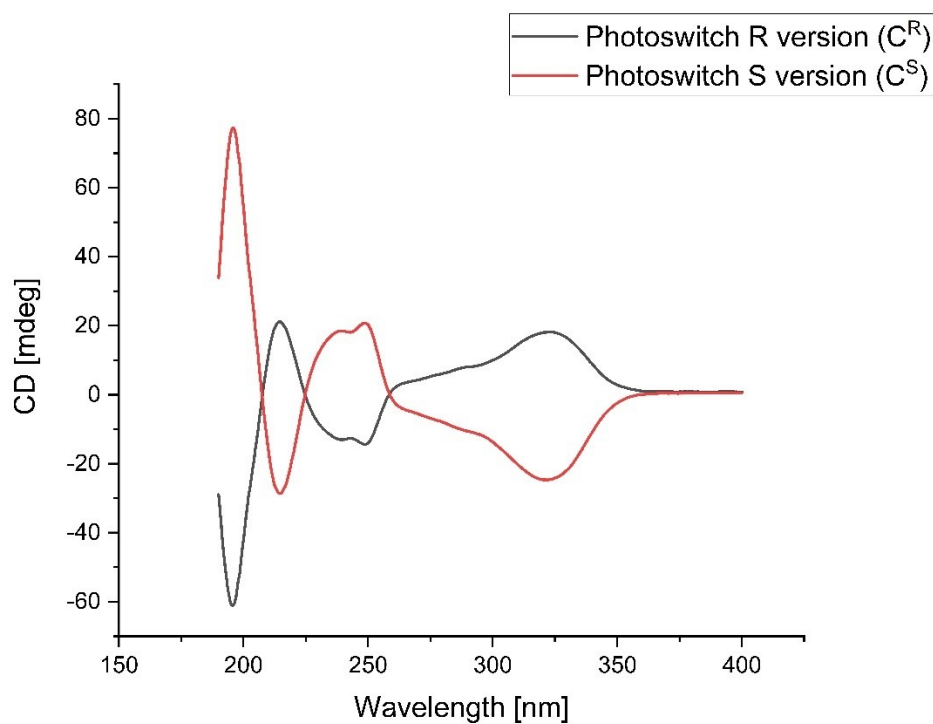
SI 53: MALDI TOF Spectra of C<sup>S</sup>-P<sub>16</sub>-E<sub>1</sub>

Using formula (1), the percentage conversion was calculated as 85%.

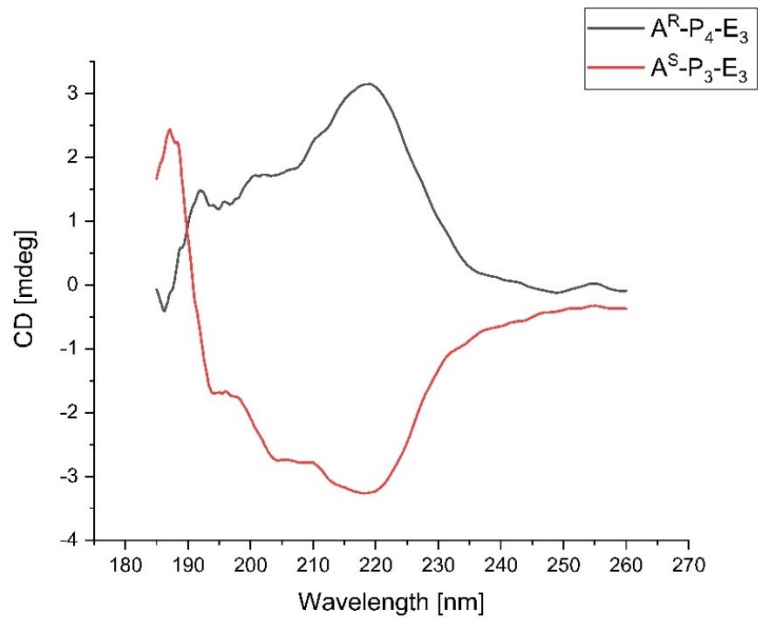


SI 54 Experimental (Black) & Simulated (Red) Isotope pattern for modified polymer  $C^S-P_{16}-E_1$  with 18 repeating units +  $Na^+$

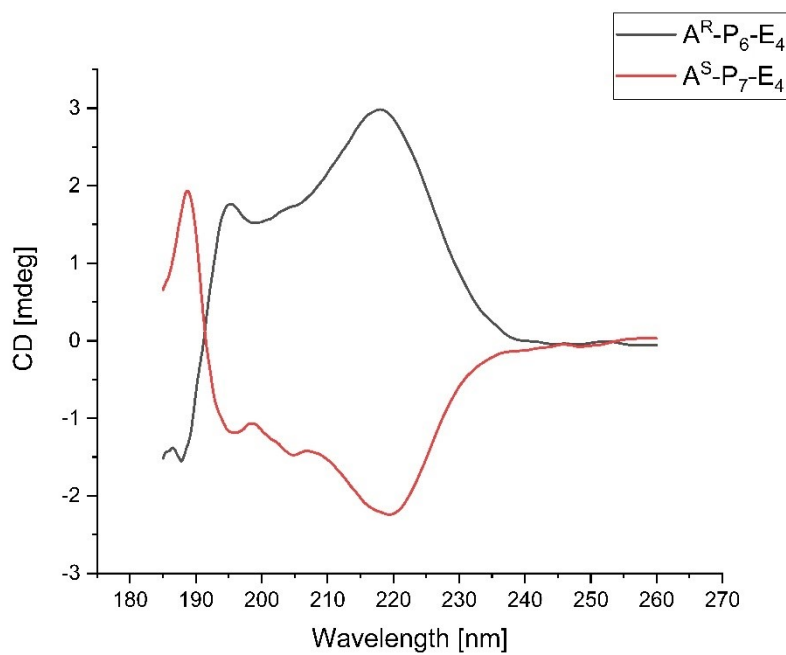
## CD Data



SI 55 : CD spectra of the photoswitch initiators  $C^R$  and  $C^S$

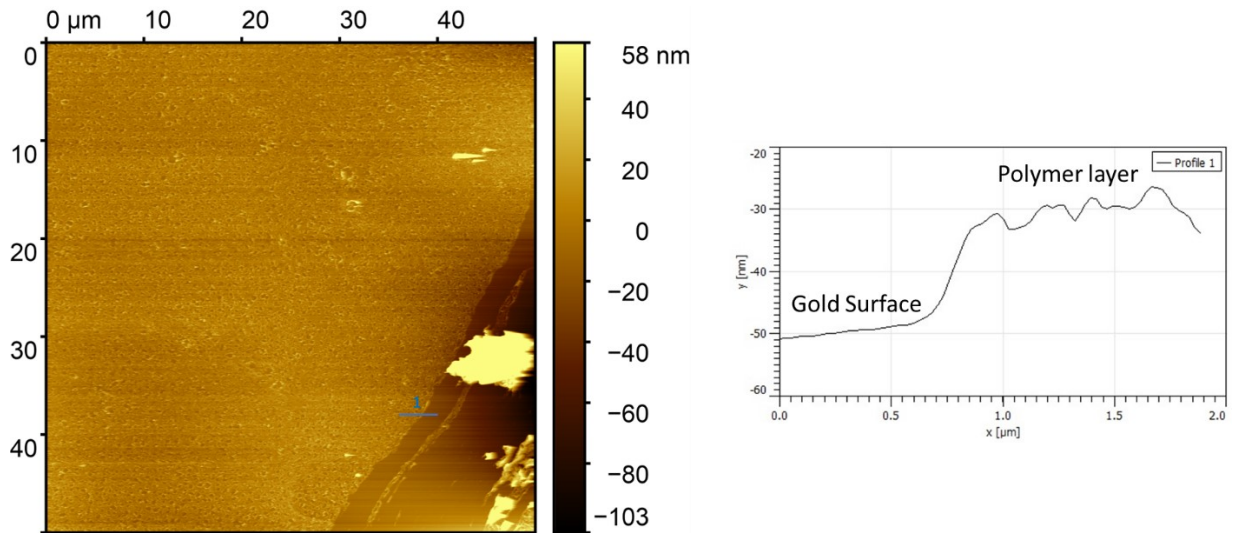


SI 56: CD spectra of the Boc-Gly-OH functionalized polymers  $A^R-P_4-E_3$  and  $A^S-P_3-E_3$



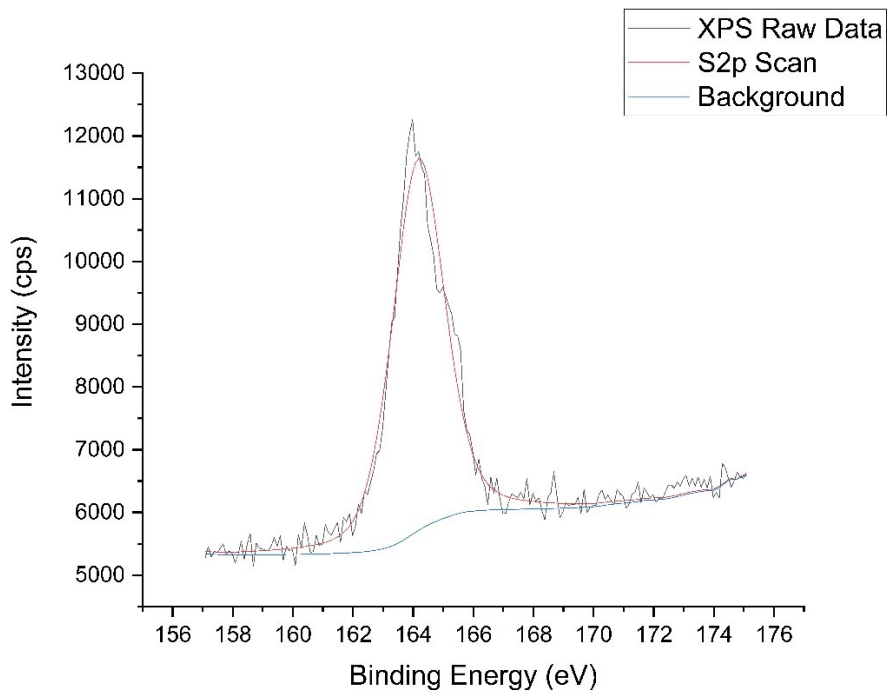
SI 57: CD spectra of the FCA functionalized polymers  $A^R-P_6-E_4$  and  $A^S-P_7-E_4$

## AFM Data

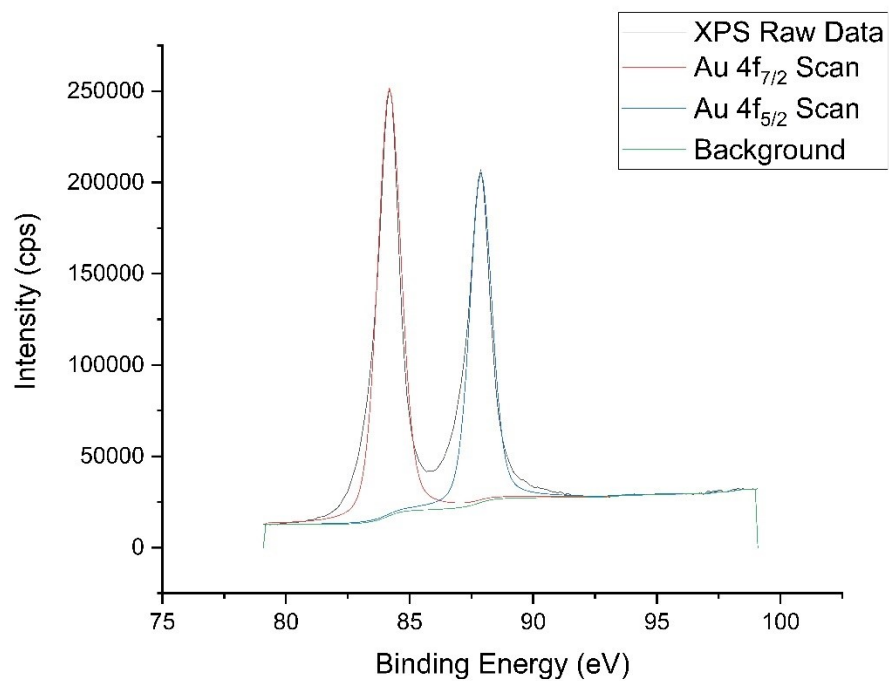


SI 58: AFM topography of the polymer-functionalized gold-surface after selective etching with HCl, revealing an exposed gold region adjacent to the polymer-covered area. The corresponding height profile across the etched boundary shows a step height of approximately 15-20 nm.

## XPS Data



SI 59 XPS S 2p spectrum of the polymer functionalized of the polymer-functionalized gold surface showing a signal at 163-164 eV.



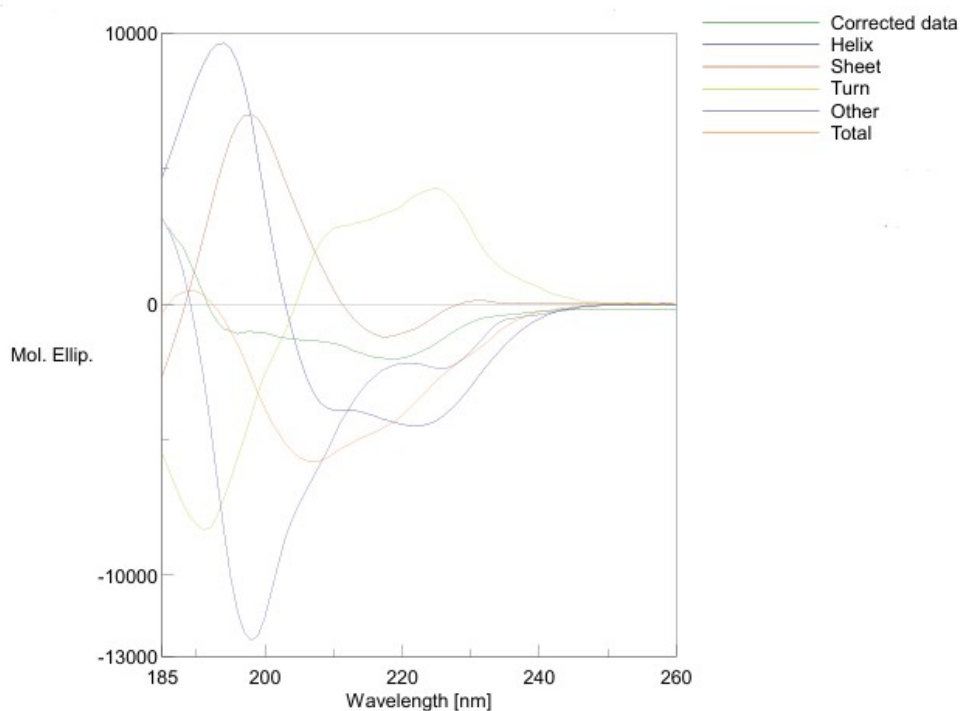
*SI 60 uncoated gold substrate showing the characteristic Au 4f doublet signal (Au 4f<sub>7/2</sub> ≈ 84 eV, Au 4f<sub>5/2</sub> ≈ 87-88 eV)*

## Workflow for Gold Substrate Coating

### CD Multivariate SSE Analysis

To further assess retention of the helical secondary structure after end-group modification, selected CD spectra were analysed using the CD Multivariate SSE program implemented in JASCO spectra manager. The analysis provides an approximate estimation of the helical content in secondary-structure contributions through comparison with reference spectral datasets. A representative fit obtained for  $A^S-P_9-E_1$  using the PCR quantitative analysis model is shown in Figure SI 62. The estimated helical-content values obtained for the analysed point-chiral and binaphthol-initiated systems before and after end-group modifications are summarized in Table 2. No significant changes in the estimated helical content were observed after modification, consistent with retention of the overall helical secondary structure indicated by the CD spectra. The corresponding analysis was not performed for the Feringa photoswitch containing systems, as the available software models were not applicable to the spectral range of the system. Since the reference databases used in these analyses do not explicitly include  $3_{10}$ -helical foldamers, therefore, the reported values should be interpreted as approximate estimation of relative helical content.

SI 61 Overall flow-scheme illustrating the coating of gold substrates with the lipoic-acid-functionalized poly(Aib) chains ( $A^R-P_9-E_1$ )



SI 62 Representative CD Multivariate SSE analysis of  $A^S-P_9-E_1$  using the PCR quantitative analysis model implemented in JASCO Spectral Manager<sup>TM</sup>. The corrected experimental spectrum together with the fitted total spectrum and the individual secondary-structure component contributions are shown.

Table 2 Estimated Secondary Structure / helical content values obtained from the CD Multivariate SSE for poly(Aib) systems before and after endgroup modifications. The values represent approximate estimations based on available reference databases.

Sample Name	Helix (%)	Sheet (%)	Turn (%)	Others (%)
A <sup>S</sup> -P <sub>0</sub> -E <sub>0</sub>	18.7	25.6	17.6	38.1
A <sup>R</sup> -P <sub>0</sub> -E <sub>0</sub>	13.5	20.3	20.1	46.1
A <sup>S</sup> -P <sub>9</sub> -E <sub>1</sub>	14.7	27.7	18.4	39.2
A <sup>R</sup> -P <sub>8</sub> -E <sub>1</sub>	11.0	37.2	18.6	33.1
B <sup>S</sup> -P <sub>0</sub> -E <sub>0</sub>	8.2	37.3	16.9	37.6
B <sup>R</sup> -P <sub>0</sub> -E <sub>0</sub>	9.7	34.6	17.6	38.1
B <sup>S</sup> -P <sub>14</sub> -E <sub>1</sub>	7.9	29.9	23.6	38.6
B <sup>R</sup> -P <sub>13</sub> -E <sub>1</sub>	9.1	33.4	15.8	41.7

## References

- (1) Freudenberg, J.; Binder, W. H. Chirality Control of Screw-Sense in Aib-Polymers: Synthesis and Helicity of Amino Acid Functionalized Polymers. *ACS Macro Letters* **2020**, *9* (5), 686-692. DOI: 10.1021/acsmacrolett.0c00218.
- (2) Rohmer, M.; Ucak, Ö.; Fredrick, R.; Binder, W. H. Chiral amines as initiators for ROP and their chiral induction on poly(2-aminoisobutyric acid) chains. *Polymer Chemistry* **2021**, *12* (43), 6252-6262. DOI: 10.1039/d1py01021b.
- (3) Van Leeuwen, T.; Gan, J.; Kistemaker, J. C. M.; Pizzolato, S. F.; Chang, M. C.; Feringa, B. L. Enantiopure Functional Molecular Motors Obtained by a Switchable Chiral-Resolution Process. *Chemistry – A European Journal* **2016**, *22* (21), 7054-7058. DOI: 10.1002/chem.201600628.